EDITORIAL

Publicity

Newspapers and magazines are printing more stories about scientific advances than ever before. The general public is slowly learning that an interest in the progress of science is essential in our modern society. A large portion of the financial support for scientific research comes from public funds. It is, therefore, the duty of the scientist to cooperate with the press and to make sure that the news articles convey the proper meaning of the discoveries and are free from exaggerated claims of importance and usefulness.

Since many of the advances in physics are first published in PHYSICAL REVIEW LETTERS, we send complimentary copies to several science writers. Moreover, we alert them in advance about potentially newsworthy papers, usually through the excellent services of Mr. Eugene Kone, Director of Public Relations for the American Institute of Physics, who has also greatly improved the handling of press conferences and releases at our meetings.

We recommend that our authors check with us or Mr. Kone on matters of press relations. As a matter of courtesy to fellow physicists, it is customary for authors to see to it that releases to the public do not occur before the article appears in the scientific journal. Scientific discoveries are not the proper subject for newspaper scoops and all media of mass communication should have equal opportunity for simultaneous access to the information. In

124083

the future, we may reject papers whose main contents have been published previously in the daily press. While we welcome the intensified interest of the layman in physics research we recognize that formerly crackpots often made the front page with their spectacular stories, and this still happens occasionally. We are sure that our authors do not wish to be confused with these pseudo-scientists in the minds of the public. This can be avoided by using the right publicity channels which will give these stories an authoritative stamp of reliability and the proper dignity. In addition, careful planning and preparation of news material will achieve increased accuracy in the interpretation of science.

S. A. Goudsmit

PHYSICAL REVIEW
LETTERS

VOLUME 4 JANUARY 1, 1960 NUMBER 1

SELF-DIFFUSION IN LIQUID He^3†

H. R. Hart, Jr.,* and J. C. Wheatley‡
Department of Physics, University of Illinois, Urbana, Illinois
(Received November 30, 1959)

The self-diffusion coefficient of liquid He^3 has been measured in the temperature range from 0.067°K to 2.97°K at pressures near the saturated vapor pressure. The results indicate that the diffusion coefficient goes through a minimum near 0.55°K and increases rapidly below 0.2°K.

The diffusion coefficient, D, was measured using the method of spin echoes.[1-3] A 90° - 180° - 180° rf pulse sequence was used with a fixed time delay between the 90° pulse and the first 180° pulse, and a variable time, τ, between the two echoes. The resulting spin echoes were displayed on an oscilloscope and photographed. The ratio, R, of the amplitudes of the two echoes is $R = \exp(-\tau/T_2 - \gamma^2 G^2 \tau^3 D/12)$, where G is the magnetic field gradient, typically 1 gauss/cm, $\gamma = 2.038 \times 10^4$ (gauss-sec)$^{-1}$, and T_2 is the transverse relaxation time, the effect of which is negligible in these experiments. An iron-free Helmholtz pair produced a resonance field, H_0, of 26.2 gauss. A Maxwell gradient pair produced, parallel to H_0, a uniform field gradient, whose magnitude was calculated from the geometry. The rf pulse amplitude, $2H_1$, was chosen small ($H_1 \cong 0.25$ gauss) in order to avoid excessive rf heating. Hence, the gradient was turned off during the duration of a pulse in order that H_1 would be much larger than the field inhomogeneity. The time τ was corrected accordingly. The signal-to-noise ratio was increased by magnetizing in a 125-gauss field which was turned off sufficiently slowly just before each diffusion measurement.

Temperatures below 1°K were obtained by the adiabatic demagnetization of approximately 75 grams of ferric ammonium alum and were measured to within about 2% by the susceptibility of 8.3 grams of cerium magnesium nitrate. Liquid He^3, 98.9% pure, was introduced through a Cu-Ni tube[4] into a 0.38-cm^3 cylindrical bulb molded of the epoxy resin, Epibond 104.[5] Thermal contact between the liquid He^3 and the two salts was obtained with a bundle of 2000 insulated copper wires, 0.0051 cm in diameter, 760 of which looped into the liquid He^3 cavity. The wire loops were rectangular, with a total length of 850 cm of wire perpendicular to the gradient and rather loosely packed next to the vertical walls of the cylinder, and with 320 cm of wire parallel to the gradient distributed vertically through the cylinder in three groups in order to inhibit convection.

The results are shown in Fig. 1. The 2.38-atmos data of Garwin and Reich[3] are shown for comparison. The diffusion measured in the spin-echo method is the diffusion of the magnetization of the nuclei. This diffusion may take place, at one extreme, by atomic diffusion, or, at the other extreme, by a spin diffusion, without atomic diffusion, due to the interaction of neighboring nuclei. Garwin and Reich, considering the magnetic dipole interaction, state that the D due to it is probably smaller than 3×10^{-12} cm^2/sec. Susceptibility measurements by Fairbank, Ard, and Walters[6] can be interpreted in terms of an exchange interaction between the spins which is large compared to the dipolar interaction. The resulting spin diffusion without

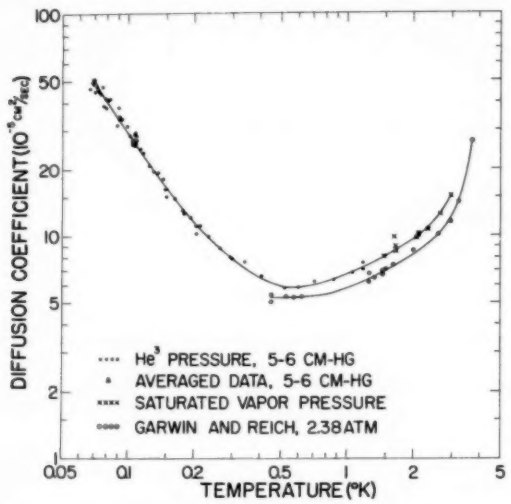

FIG. 1. Logarithm of the self-diffusion coefficient of liquid He^3 vs the logarithm of the temperature. The two triangles each represent the average of six data points too closely spaced to be shown separately. The data of Garwin and Reich are taken from reference 3.

atomic diffusion is still too small to account for the experimental results. Hence it is very likely that the increase of D at low temperatures is caused by a decreased probability of scattering of atoms, or groups of atoms, moving through the liquid. This decreased scattering was predicted for the elementary excitations of liquid He^3 by Pomeranchuk[7] and, more quantitatively, by Landau.[8] Experimental measurements of D by Garwin and Reich down to 0.45°K and of the thermal conductivity by Fairbank and Lee[9] down to 0.2°K give no indication of this effect. However, measurements[10] of the viscosity by Zinov'eva down to 0.35°K show an increase in the temperature dependence at the lowest temperatures. This fact has been interpreted by Abrikosov and Khalatnikov[8] as evidence for the decreased scattering at low temperatures. It should be noted that the effective nuclear interactions mentioned above may decrease the magnetization diffusion relative to the atomic diffusion in our experiments.

The values of D in Fig. 1 were derived neglecting T_2 decay, convection, residual field gradients, and artificial diffusion barriers. These possible sources of error will now be discussed. (*i*) Measured lower limits on T_2 are 0.55 second at 0.072°K, 1.5 seconds at 0.18°K, and longer at higher temperatures. The resultant systematic error in D is less than +1.5%. (*ii*) Convection was produced intentionally at 1.75°K by changing the temperature at a rate $\dot{T} = 0.018$°K/sec. The effective D in this case was 14×10^{-5} cm²/sec compared with 9×10^{-5} cm²/sec for $\dot{T} < 10^{-6}$ °K/sec. Near 1°K the difference between D for $\dot{T} = 3.6\times10^{-4}$ °K/sec and D for $\dot{T} < 10^{-5}$ °K/sec was negligible. These results, together with convection theory[11] and the properties of He^3,[12] indicate that the error due to convection is negligible at our usual values of $\dot{T}$, less than 5×10^{-5} °K/sec. (*iii*) D was measured as a function of the polarity and magnitude of the field gradient G and no systematic changes of D with G were observed in the relevant region of G. (*iv*) The cooling wires and bulb walls limit the diffusion of some of the He^3 atoms, lowering the measured value of D. The He^4 impurities also lower the value of D relative to that of pure He^3.[13] Since both of these effects increase with D, they decrease the temperature dependence of D at low temperatures, which, in the present experiment, is $T^{-3/2}$ at 0.08°K. The decrease in the measured values of D due to the boundaries is probably a few percent at the low temperatures, but it cannot be estimated quantitatively.

We would like to thank Professor John Bardeen, Dr. R. L. Garwin, and Dr. D. W. McCall for helpful discussions; W. F. Carlock, F. F. Jurkovich, and R. J. Sarwinski for help in performing the experiment and processing the data; and G. L. Salinger for translating several Russian articles.

†This work has been supported by the Alfred P. Sloan Foundation, the U. S. Atomic Energy Commission, and the Office of Naval Research. It is being submitted by H. R. Hart, Jr., in partial fulfillment of the requirements for the Ph.D. degree, University of Illinois.

*U. S. Steel Foundation Fellow.

‡A. P. Sloan Fellow.

[1]E. L. Hahn, Phys. Rev. 80, 580 (1950).

[2]H. Y. Carr and E. M. Purcell, Phys. Rev. 94, 630 (1954).

[3]R. L. Garwin and H. A. Reich, Physica 24, S133 (1958); Phys. Rev. 115, 1478 (1959). We are indebted to them for sending us a preprint of their paper.

[4]This tube, 70% copper and 30% nickel, became slightly magnetic at low temperatures.

[5]Furane Plastics, Inc., 4516 Brazil Street, Los Angeles 39, California.

[6]Fairbank, Ard, and Walters, Phys. Rev. 95, 566 (1954).

[7]I. Ia. Pomeranchuk, J. Exptl. Theoret. Phys. U.S.S.R. 20, 919 (1950).

[8]L. D. Landau, J. Exptl. Theoret. Phys. U.S.S.R. 30, 1058 (1956)[translation: Soviet Phys. JETP 3, 920 (1957)]. See also, A. A. Abrikosov and I. M. Khalatnikov, Reports on Progress in Physics (The Physical Society, London, 1959), Vol. 22, p. 329.

[9]H. A. Fairbank and D. M. Lee, Symposium on Solid and Liquid Helium Three, 1957 (Ohio State University Press, Columbus, 1958), p. 26.

[10]K. N. Zinov'eva, J. Exptl. Theoret. Phys. U.S.S.R. 34, 609 (1958) [translation: Soviet Phys. JETP 7, 421 (1958)].

[11]O. A. Saunders, Proc. Roy. Soc. (London) A172, 55 (1939).

[12]V. P. Peshkov and K. N. Zinov'eva, Reports on Progress in Physics (The Physical Society, London, 1959), Vol. 22, p. 504; D. M. Lee and H. A. Fairbank, Phys. Fluids 2, 582 (1959); K. A. Brueckner and K. R. Atkins, Phys. Rev. Letters 1, 315 (1958); D. F. Brewer and J. G. Daunt, Phys. Rev. 115, 843 (1959).

[13]V. N. Zharkov and V. P. Silin, J. Exptl. Theoret. Phys. U.S.S.R. 37, 143 (1959).

DOPPLER-SHIFTED CYCLOTRON FREQUENCY RADIATION FROM PROTONS IN THE EXOSPHERE

W. B. Murcray and J. H. Pope
Geophysical Institute, University of Alaska, College, Alaska
(Received November 12, 1959)

In a recent publication[1] MacArthur has suggested that the phenomenon known as "Dawn chorus" may be due to Doppler-shifted radiation from protons which are rotating about the lines of force of the earth's magnetic field with the cyclotron frequency: $\nu_C = 1.54\times10^3 B$, where B is the field strength in gauss. The suggestion is quite attractive, because it involves a simple physical process, and because if it should prove correct, examination of the dispersion curves of the chorus radiation might furnish considerable information about the outer ionosphere. Accordingly, it seems worthwhile to investigate the suggestion in more detail.

The cyclotron frequency for protons in the earth's field is below 10^3 cps everywhere, and the frequencies observed in chorus reach several times this value. From this it is evident that the Doppler shift must be large, corresponding to protons with radial velocities very near the local velocity of electromagnetic radiation. The actual proton velocities, however, are low and consequently one is justified in neglecting the term in β^2 in the Doppler-shift equation

$$\nu' = \nu_0(1-\beta^2)^{1/2}/(1-\beta n).$$

Here ν' is the Doppler-shifted frequency, ν_0 is the proton gyrofrequency, and β is given by $\beta = V/c$, where V is the radial component of the velocity of approach of the particle, c is the velocity of light in free space, and n is the index of refraction for the frequency ν_0 (in the extraordinary mode). For frequencies of the order of a thousand cps the index of refraction is closely approximated by $n = (1+80.5N\times10^6/\nu_e\nu)^{1/2}$, where N is the electron density in electrons cm^{-3} and ν_e is the electron gyrofrequency.

A group of protons entering the earth's field at velocity V will then emit the Doppler-shifted frequency:

$$\nu' = \nu_c \Big/ \left[1 - \frac{V}{c}\left(1 + \frac{80.5N\times10^6}{\nu_e\nu_c}\right)^{1/2}\right],$$

which will vary with the magnetic field strength (through ν_e), electron density, and particle speed. Whether or not the mechanism discussed can be considered as a possible source of chorus depends in part upon whether or not it can produce the proper frequency-time curve. Consideration of the various factors involved makes it seem likely that the most promising region where this might occur is the outer ionosphere. Accordingly, a model frequency-time curve for protons entering the earth's field at a radial velocity of 10^3 km sec^{-1} at a geomagnetic latitude of 65° has been calculated and is shown in Fig. 1. The maximum ion density is assumed to be 10^6 cm^{-3} at 300 km height and above this to follow an exponential distribution $N = N_0 e^{-0.0032h}$ (h is the distance in kilometers above the 300-km level). This corresponds to a scale height of a little over 300 km and is quite close to the model quoted by Johnson,[2] and is thought to be reasonable for the top of the ionosphere above College, Alaska. For the frequencies of interest here, the travel times through the ionosphere are quite long and have a considerable effect on the shape

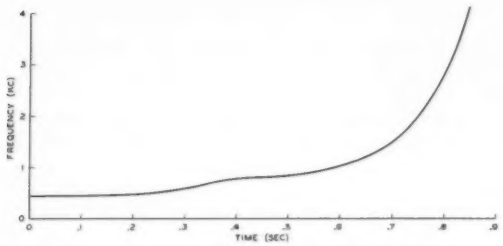

FIG. 1. Theoretical chorus dispersion curve.

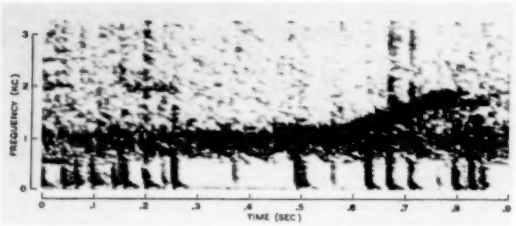

FIG. 2. Audio spectrogram of chorus.

of the final frequency-time curve; the curve shown in Fig. 1 has been corrected for travel times, and represents what would be received on the ground.

It is evident that one can get almost anything in the way of a frequency-time curve, by the proper choice of electron density distribution. However, the use of probable distributions appears to explain many of the chorus dispersion curves actually encountered. This mechanism would also account for the hiss often associated with chorus.

Chorus as observed at College usually is in the frequency range of 1 kc/sec to 4 kc/sec although it is occasionally observed below 1 kc/sec and above 10 kc/sec. The individual components generally are ascending tones beginning at about 1 kc/sec and ending at 3 to 4 kc/sec, 0.2 to 0.5 sec later.

The dispersion curve of chorus bears considerable resemblance to that shown in Fig. 1 (see Fig. 2). It sometimes shows a linear frequency-time curve but often begins in a concave upward curve as in Fig. 1. Its termination, however, is often a slightly concave downward curve not indicated in the figure which might be accounted for by a slowing down of the particles as they approach absorption or by their passing through a maximum of ion density. A study of the variations in the characteristics of chorus with the properties of the ionosphere might help to reject or confirm this hypothesis.

This research was partially supported by Air Force Cambridge Research Center.

[1]J. W. MacArthur, Phys. Rev. Letters 2, 491 (1959).

[2]Francis S. Johnson, Lockheed Technical Report LMSD 49719, April, 1959 (unpublished).

QUESTION OF THE EXISTENCE OF A LUNAR MAGNETIC FIELD*

Marcia Neugebauer
Jet Propulsion Laboratory, California Institute of Technology, Pasadena, California
(Received November 30, 1959)

Soon after their recent moon-impact, scientists of the U.S.S.R. announced[1] that the magnetometer on the vehicle had detected no evidence of a lunar magnetic field; their instrument was capable of detecting fields down to 6×10^{-4} gauss. The impact occurred on the sunlit side of the moon. The final magnetometer reading before impact presumably was obtained at a lunar altitude of the order of a kilometer, or more.

It is the purpose of this note to point out that this single piece of data is not sufficient evidence from which to conclude that the general lunar magnetic field is weaker than 6×10^{-4} gauss on the surface. It is suggested that, if a general lunar magnetic field existed, it would be confined by the solar corpuscular radiation, or solar wind, to a thin layer above the sunlit surface, but it could extend a considerable distance beyond the surface on the side away from the sun.

An upper limit to the strength of magnetic field which can be pushed around by the solar wind can be obtained by a calculation of the momentum of the solar corpuscular radiation. If it is assumed that the proton density, n, is 500 cm^{-3} and that the average particle velocity, v, is 1000 km/sec, the momentum flux per unit area, or pressure, in the solar wind is $nMv^2=8\times10^{-8}$

dynes/cm^2. A pressure of this magnitude is capable of compressing a magnetic field until the magnetic pressure, $B^2/8\pi$, builds up to this size; the magnetic-field strength corresponding to this pressure equals $(8\pi \times 8 \times 10^{-6})^{1/2} = 1.4 \times 10^{-2}$ gauss.

Recent observations by Kozyrev and by Dubois (see a recent publication by Kopal[2]) of both the energy content and the time variations of the luminescence of some parts of the lunar surface indicate that this luminescence is, in large part, caused by solar corpuscular radiation incident on the lunar surface rather than by solar electromagnetic radiation. As the luminescence is observed only in sunlit regions of the lunar surface, it can be argued that the solar corpuscular radiation must have travelled essentially straight into the moon's surface without being appreciably deflected by either a lunar or an interplanetary magnetic field. According to the argument in the preceding paragraph, the solar corpuscular radiation could not have reached the lunar surface if the moon's surface magnetic-field strength were greater than $\sim 10^{-2}$ gauss.

These observations and their interpretation are consistent with the estimates of the strength of a possible lunar magnetic field based on various theories of the formation and history of the moon; these estimates[3] range from zero to several hundred gamma (1 gamma $= 10^{-5}$ gauss).

Let it be supposed that, in the absence of the solar wind, the lunar magnetic field (B_0) would be a few hundred gamma or less on the surface. The protons and electrons in the solar corpuscular radiation are deflected by this field so as to set a current; the field resulting from this current tends to cancel the moon's field above the lunar surface and to add to it below the surface. The equilibrium properties of such a magnetic boundary layer can be calculated for the case of a cold plasma normally incident on a one-dimensional "moon" from the equations for such a plasma given by Davis, Lüst, and Schlüter.[4] If all the dependent variables but the magnetic-field strength are eliminated from these equations, there results the differential equation

$$\frac{d}{dx}\left[(1-\beta^2)\frac{d\beta}{dx}\right] = \frac{4\pi e^2 n}{m}\beta,$$

where

$$\beta^2 = \frac{1}{nMv^2}\frac{B^2}{8\pi}.$$

Also, M and m are the proton and electron masses, respectively, and x is the distance from the lunar surface (measured negatively out from the surface in order that the plasma flow is in the positive x direction). This equation can be solved subject to the boundary conditions that the magnetic-field strength is $2B_0$ at the surface of the "moon" and zero at $-\infty$, with the result that

$$(4\pi e^2 n/m)^{1/2} x = -\left[\left[1 - \tfrac{1}{2}(\beta^*)^2\right]^{1/2} - (1 - \tfrac{1}{2}\beta^2)^{1/2} + \ln(\beta^*/\beta) + \ln\frac{1 + (1 - \tfrac{1}{2}\beta^2)^{1/2}}{1 + [1 - \tfrac{1}{2}(\beta^*)^2]^{1/2}}\right],$$

where

$$(\beta^*)^2 = \frac{1}{nMv^2}\frac{(2B_0)^2}{8\pi}.$$

For small values of β, ($B_0 \ll 7 \times 10^{-3}$ gauss), this expression can be approximated by

$$B = 2B_0 \exp\left[-\left(\frac{4\pi e^2 n}{m}\right)^{1/2} x\right] = 2B_0 e^{-4.2x(\text{km})}$$

Thus, if the moon had a surface field strength of less than ~ 700 gamma in the absence of the solar wind, the field would, according to this model, drop to $1/e$ of this value at ~ 500 meters above the surface on the sunlit side; this height is much less than the altitude of many of the lunar mountains. For an undistorted surface field as large as 700 gamma, the transverse displacement of the protons is only 8 meters.

This model is not completely realistic in many ways: For a three-dimensional moon, the current layer is curved; thus, the field strength at the surface is not exactly $2B_0$. Furthermore, the solar corpuscular radiation is not a cold plasma and, thus, a random velocity distribution will be superimposed on the flow previously described. Collisions between particles in the plasma were neglected; however, the mean free path for large-angle collisions is orders of magnitude greater than the calculated boundary-layer thickness. All reflection of charged particles from the lunar surface has been neglected, as has any contribution from the solar magnetic field which may be trapped in the solar corpuscular radiation. Furthermore, a steady-state solution was found and all plasma oscillations were ignored. It is believed that corrections for these effects would either be small or would lead to a smaller boundary-layer thickness than that calculated.

The author would like to thank Dr. L. Davis

for his interest in and assistance with this problem.

*This work was sponsored by the National Aeronautics and Space Administration.

[1]"Preliminary Results of Data Processing from the Second Soviet Cosmic Rocket," Jet Propulsion Laboratory, Pasadena, California, October 23, 1959, JPLAI/Translation No. 12 (translated by J. L. Zygielbaum from Pravda and Izvestia, September 18-23, 1959).

[2]Z. Kopal, "Does the Moon Possess a Magnetic Field?," Space Journal, September, 1959 (p. 3).

[3]E. H. Vestine, "Utilization of a Moon-Rocket System for Measurement of the Lunar Magnetic Field," RAND Corporation Report RM-1933, July 9, 1957 (unpublished).

[4]Davis, Lüst, and Schlüter, Z. Naturforsch. 13a, 916 (1958).

DETERMINATION OF THE AGE OF THE ELEMENTS*

J. H. Reynolds
Miller Institute for Basic Research in Science and Department of Physics,
University of California, Berkeley, California
(Received December 7, 1959)

We have found that xenon from the chondritic (stone) meteorite Richardton is heavily enriched in Xe^{129}. This isotope almost certainly was formed from the radioactive decay of I^{129}, now extinct as a natural radioactivity but not so at the time of formation of the meteorite. From the data we calculate that $(0.35 \pm 0.06) \times 10^9$ years elapsed between the time of formation of the elements and the meteorite. There is a large body of evidence that the chondrites were formed at a time close to 4.6×10^9 years ago. Thus the age of the elements is close to 4.95×10^9 years.

In 1947, Brown[1] suggested that the meteorites could be used to determine quite accurately the age of the elements if the daughter of an extinct natural radioactivity could be found there. The decay

$$I^{129} \xrightarrow{1.7 \times 10^7 \text{ yr}} Xe^{129}$$

has long been recognized as a particularly favorable case for stone meteorites, although previous searches for fossil Xe^{129} in the chondrite Beardsley[2] and the achondrite Nuevo Laredo[3] failed to give a positive result.

Figure 1 is a faithful tracing of the peak heights recorded with a sensitive mass spectrometer[4] during one of the sweeps of the spectrum of xenon which had been extracted from the vacuum melting of a 7-gram sample of Richardton. The horizontal lines drawn through the various peaks show where the peaks would fall for an analysis, under identical conditions, of a sample of atmospheric xenon[5] having the same Xe^{132} content. Differences between the two spectra, notably the large Xe^{129} excess in the meteoritic sample, are very obvious from the figure. A sequence of runs on four independently prepared xenon samples from this meteorite, interspersed with runs on atmospheric xenon, have established beyond any possible doubt

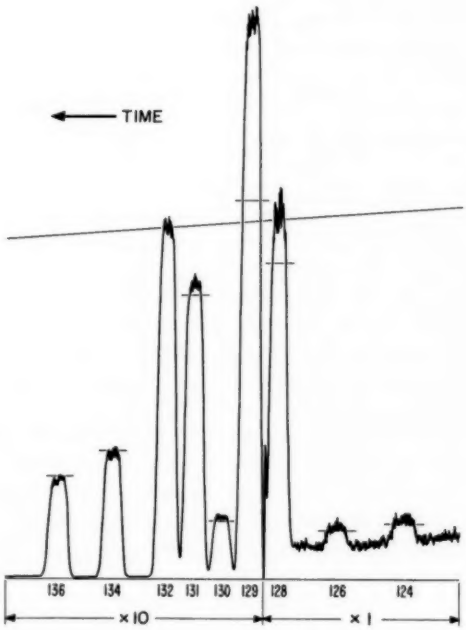

FIG. 1. Mass spectrum of Xe extracted from Richardton stone meteorite and sealed off in the mass spectrometer. Horizontal lines show the comparison spectrum of terrestrial Xe. The slant line through the 132 peak shows the extent of spectrometer pumping. Jagged peak tops are due to statistical fluctuations in the small ion currents.

that all of the differences seen in Fig. 1—including those at the rare masses 124 and 126—are real and are not due to such extraneous effects as chemical impurities, spectrometer "ghost" peaks, spectrometer memory from previous anomalous xenon samples (there had been none in this instrument), or instrumental instability. For example we have plotted in Fig. 2 both the meteoritic xenon spectrum and a spectrum from a sample of atmospheric xenon of the same size, the points normalized to the atmospheric abundances in both cases. In these two plots, mean deviations are indicated whenever they exceed the size of the points.

It will be noted in Fig. 2 that 136 is the least abundant isotope in the meteorite relative to atmospheric abundances. Accordingly, for the purposes of the calculations in this Letter, it has been assumed that the Xe^{136} in the sample of xenon from the meteorite is an index to the xenon of terrestrial composition in the sample, whether by contamination from the atmosphere or otherwise. The isotopic composition of the xenon from the meteorite, after this terrestrial component has been subtracted, appears in Table I. The errors quoted are mean deviations.

A Xe^{128} spike was used to determine the amounts of xenon in the meteorite. Care was taken not to introduce spiked samples into either the extraction apparatus or the mass spectrometer until all questions about the unspiked isotopic composition had been settled. Solid KI which had been outgassed in vacuum, finely powdered, and then briefly irradiated in a pile was the means by which the small amounts of tracer Xe^{128} required were handled. The results of the isotopic dilution analysis appear in Table I. One gram of Richardton contains 13×10^{-11} cc STP of excess Xe^{129}. This disagrees with the conclusions of Wasserburg and Hayden[2] who found an upper limit of 1.3×10^{-11} cc STP/g in the Beardsley meteorite.

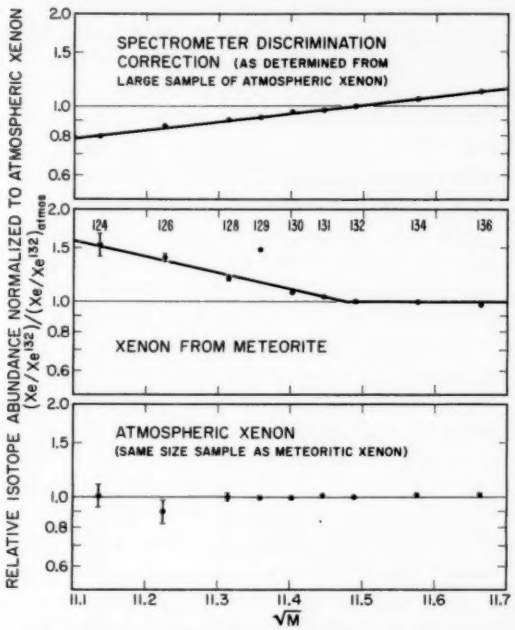
RELATIVE ISOTOPE ABUNDANCE NORMALIZED TO ATMOSPHERIC XENON
$(Xe/Xe^{132})/(Xe/Xe^{132})_{atmos}$
SPECTROMETER DISCRIMINATION CORRECTION (AS DETERMINED FROM LARGE SAMPLE OF ATMOSPHERIC XENON)
XENON FROM METEORITE
ATMOSPHERIC XENON
(SAME SIZE SAMPLE AS METEORITIC XENON)
124 126 128 129 130 131 132 134 136
$\sqrt{M}$

FIG. 2. Relative isotope abundance normalized to atmospheric xenon. $(Xe/Xe^{132})/(Xe/Xe^{132})_{atmos}$.

The presence of isotopes other than 129 in the anomalous spectrum probably means that other nuclear processes, induced by cosmic-ray bombardment, have contributed to the xenon in Richardton. This raises the question of whether the Xe^{129} might have been produced by some means other than the decay of extinct I^{129}. Quite aside from the difficulties involved in accounting for so much Xe^{129} production from the limited number of heavy-target nuclei available in the meteorite, strong arguments based on the isotopic composition of the anomalous xenon can be advanced against such mechanisms dominating the Xe^{129} production. Of particular importance

Table I. Xe from sample *KA* 382-2*H*: 6.69 g of Richardton, 20-100 mesh.

	Isotopic composition of anomalous component								
Isotope	124	126	128	129	130	131	132	134	136
Percent abundance	0.33±0.09	0.23±0.02	2.5±0.3	81.5±3.5	2.3±0.4	8.2±2.0	3.6±2.3	1.4±1.0	≡0

Xenon of terrestrial composition: $(0.88\pm0.05)\times10^{-9}$ cc STP/g

Xenon of anomalous composition: $(0.16\pm0.01)\times10^{-9}$ cc STP/g

in this connection is the fact that in the anomalous component, Xe^{129}/Xe^{131} is 10.0. Table II lists various possible mechanisms for Xe^{129} production with the Xe^{129}/Xe^{131} ratio expected in each case. None fit the observations. We are forced to conclude that I^{129} decay has produced the bulk of the Xe^{129}.

The time interval between nucleogenesis and the formation of the meteorite is given by

$$\Delta t = \frac{1.72\times 10^7}{0.693}\left[\ln(I^{127}/Xe^{129})_{met} + \ln(I^{129}/I^{127})_0\right] \text{ years.}$$

We assume that $(I^{129}/I^{127})_0 = 1$, i.e., that I^{129} and I^{127} were produced initally in equal amounts. Analytical data on I in chondrites are poor. Suess and Urey[6] adopt 0.66 ppm, but this could be wrong by a factor of 10 for any particular meteorite. We used 1 ppm in the calculation. This leads to $\ln(I^{127}/Xe^{129})_{met} = 14.1$ and $\Delta t = 0.35\times 10^9$ years. Fortunately, an error of a factor of 10 in either $(I^{127})_{met}$ or $(I^{129}/I^{127})_0$ leads to only a 16% error in Δt.

Now that the presence of radiogenic I^{129} in meteorites has been established, the I-Xe method of dating meteorites should assume importance. It has the unique advantage that it dates meteorites from the beginning of the solar system rather than from the present.

One curious feature of the isotopic composition of the anomalous xenon component should be mentioned. This is the fact that, excluding I^{129}, the abundances of the 5 lightest isotopes fit a smooth curve when normalized to the abundances of atmospheric xenon. In Fig. 2, these normalized abundances have been plotted logarithmically against $\sqrt{M}$ and give a straight line. (This is not an instrumental effect but is in addition to the rather strong mass discrimination of the spectrometer arising from the magnetically unshielded electron multiplier. This correction, also plotted in Fig. 2, has already been applied.) This raises the possibility that the anomalies at masses 124-131 may not be due to nuclear processes at all, but may be due to a strong mass fractionation of meteoritic xenon relative to terrestrial xenon—such as might occur if terrestrial xenon is the final residue of gas which has mostly escaped from a gravitational field at some time during its history. The heavy isotopes 132, 134, and 136 do not fit the pattern. It is conceivably significant that these are the chief isotopes produced in slow-particle and spontaneous fission. In fact, the meteoritic spectrum can be decomposed quite well into a "fractionated" terrestrial component (including masses 132, 134, and 136) plus a fission xenon spectrum. Of course, presence of atmospheric contamination in the meteoritic sample would alter the composition of the "fission" xenon deduced in this way.

Table II. Possible mechanisms for Xe^{129} production.

Mechanism	(Xe^{129}/Xe^{131})
Slow-particle or spontaneous fission	<1
Fast-particle fission	>1 but ~1[a]
Spallation reactions on Cs, Ba, or heavier elements	<1 but ~1
Natural neutron capture in Te	3[b]
Observed	10.0

[a]P. C. Stevenson et al., Phys. Rev. 111, 886 (1958).

[b]M. Inghram and J. H. Reynolds, Phys. Rev. 78, 822 (1950).

I wish to thank Mr. Sidney Putnam for assistance with the laboratory work and Dr. Maynard Michel for a helpful discussion. The meteorite sample (Museum No. 100.69) was obtained from Dr. H. H. Nininger of the Meteorite Museum, Sedona, Arizona, by Professor J. E. Evernden to whom thanks are also due.

*Work supported in part by the U. S. Atomic Energy Commission.

[1]H. Brown, Phys. Rev. 72, 348 (1947).

[2]G. Wasserburg and R. Hayden, Nature 176, 130 (1955).

[3]J. H. Reynolds and J. Lipson, Geochim. Cosmochim. Acta 12, 330 (1957).

[4]J. H. Reynolds, Rev. Sci. Instr. 27, 928 (1956).

[5]A. Nier, Phys. Rev. 79, 450 (1950).

[6]H. Suess and H. Urey, Revs. Modern Phys. 28, 53 (1956).

RECOMBINATION RADIATION FROM HOT ELECTRONS IN SILICON

L. W. Davies*
Bell Telephone Laboratories, Murray Hill, New Jersey
(Received November 16, 1959)

It has been known for many years that Ohm's law ceases to hold in semiconductors as the electric field strength is increased.[1] The observed decreases in electron and hole mobilities are attributed[2] to an increase in the mean energy of the charge carriers above the equilibrium value; the carriers become heated in order that the energy gained from the electric field may continue to be dissipated by collisions with lattice vibrations.

In the experiments described here, the intensity distribution in the band-to-band recombination radiation from silicon was measured under hot electron conditions. The spectrum reflects the energy distributions of electrons and holes if recombination takes place directly; however, if an electron and hole first form an exciton, which decays with emission of the observed radiation, the spectral distribution is determined by the energy distribution of the excitons. The results to be described below indicate that the latter is the case.

The high injection levels required for adequate intensity of the recombination radiation have been achieved with diffused p-π-n[3] silicon diode structures, biased strongly in the forward direction with current densities up to 10^4 amp cm^{-2}. The electric field in the π region reached several kv cm^{-1}, with a substantially uniform distribution of injected charge density and field for sufficiently thin π regions. At these high power levels operation on a microsecond pulse basis is essential, with the diode mounted in good thermal contact with a heat bath; this in turn requires the use of a radiation detection system with time-resolution sufficient to differentiate between radiation emitted from hot and from cold electrons, respectively, during and immediately after the pulse of diode current.

The recombination radiation passed through a quartz prism spectrometer, and was detected by a 7102 infrared photomultiplier cooled by liquid nitrogen. With a suitable gating technique, only those pulses were counted which corresponded to the liberation of photoelectrons from the 7102 cathode by radiation emitted by the diode during some portion of the current pulse (duration 1.5 μsec).

Normalized spectral distributions for two extreme values of the current through one sample (2 amp and 40 amp) are shown in Fig. 1; the diode mount was at the temperature of liquid nitrogen. The results shown have been corrected for the spectral response of the system, and for absorption of radiation in the sample. The spectral resolution is indicated by the half-intensity width of Hg line radiation. At currents of 2 amp and 40 amp the field strengths were determined from the voltage across the diode to be 200 v cm^{-1} and 4 kv cm^{-1}, with injected carrier densities estimated, respectively, as 10^{17} and 10^{18} cm^{-3}. The lifetime at 77°K was found[4] to be 9×10^{-8} sec, giving a diffusion length $\sim3\times10^{-3}$ cm comparable with the diode π-region width 4.3×10^{-3} cm.

More detailed observations on several samples showed structure in the spectrum at energies less than $h\nu_0$ in Fig. 1, where $h\nu_0$ is the energy gap minus the energy of the optical phonon associated with the direct radiative transition. The radiation observed at frequencies less than ν_0

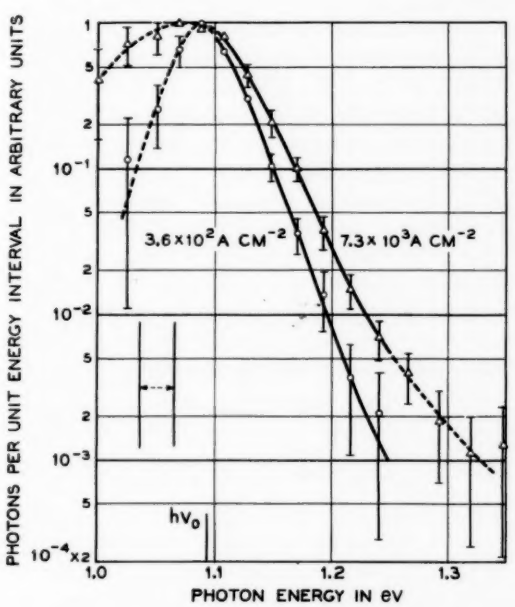

FIG. 1. Spectrum of recombination radiation from pulsed silicon p-π-n diode at 77°K.

was consequently believed to arise from extrinsic radiative recombination of charge carriers with unionized donors and acceptors at the boundaries of the diode π region.

The spectrum taken at 4 kv cm^{-1} shows a broadening to higher energies, which will be shown to be related to Joule heating in the sample. In order to determine the carrier temperature T at 4 kv cm^{-1}, in the case that electrons and holes recombine directly, we assume that the intensity N_ν (photons per unit energy interval) is given by a formula due to Lax,[5] summed over the various phonon contributions:

$$N_\nu \propto \sum_i (1-\nu_{0i}/\nu)\exp(-h\nu/kT),$$

where $h\nu_{0i}$ is the energy of the photon emitted when an electron and hole of zero thermal kinetic energy recombine through the ith phonon process. On the other hand, if the electrons and holes first form excitons, which decay with the emission of the observed radiation, then

$$N_\nu \propto \sum_i (\nu-\nu_{0i})^{\nu/2}\exp(-h\nu/kT),$$

where T is now the temperature of the excitons. In either case, a comparison of two spectra at the same lattice temperature, but with differing carrier or exciton temperatures T_1 and T_2, yields

$$(N_{\nu 1}/N_{\nu 2}) = \exp[-(h\nu/k)(T_1^{-1} - T_2^{-1})].$$

The two full curves in Fig. 1 are related in this way; on the assumption that the carriers and excitons are in equilibrium with the lattice in the low-field case ($T_1 = 77$°K), we find a value $T_2 = 83$°K at 4 kv cm^{-1}. A monotonic increase in T with diode current was found between the extreme values of Fig. 1.

A calculation was subsequently made of the Joule heating in the diode, on the assumption that the pulse energy was adiabatically and uniformly dissipated in the π region during the 1.2-μsec time interval before observation was made at a current of 40 amp, and that the sample returned to the temperature of the Dewar between pulses. A temperature rise of 7°K was determined, which coincides almost exactly with the heating measured spectroscopically.

Measurements[6] of drift velocity in n-type Si at 77°K show a decrease in mobility at fields above 700 v cm^{-1}; a comparison of this result with calculations[7] made for Ge leads to the belief that the carrier temperature in these experiments at 4 kv cm^{-1} is at least twice the lattice temperature. Since no broadening of the recombination spectrum is observed here under hot electron conditions (other than the small amount associated with Joule heating), we must conclude that the recombination radiation arises substantially from excitons in Si at 77°K, and that these excitons have a thermal distribution of energies at the lattice temperature.

Evidence for the formation of excitons in silicon at low temperatures, by absorption of radiation, has been previously presented.[8,9]

It is a pleasure to acknowledge the assistance of A. R. Storm, Jr. with the experiments, and the benefit of discussions with many members of the Laboratories, particularly J. R. Haynes.

---

*On leave from Division of Radiophysics, Commonwealth Scientific and Industrial Research Organization, Sydney, Australia, during the tenure of a Commonwealth Fund Fellowship.

[1]For a review of the experimental data, see J. B. Gunn, Progress in Semiconductors 2, 211 (1957).

[2]W. Shockley, Bell System Tech. J. 30, 990 (1951).

[3]The π layer is weakly doped p-type material containing $\approx 10^{14}$ acceptors/cc.

[4]S. R. Lederhandler and L. J. Giacoletto, Proc. Inst. Radio Engrs. 43, 478 (1955).

[5]Haynes, Lax, and Flood, J. Phys. Chem. Solids 8, 392 (1959).

[6]J. Bok, thesis, Université de Paris, 1959 (unpublished).

[7]R. Stratton, J. Electronics and Control 5, 157 (1958).

[8]Macfarlane, McLean, Quarrington, and Roberts, J. Phys. Chem. Solids 8, 388 (1959).

[9]Zwerdling, Roth, and Lax, J. Phys. Chem. Solids 8, 397 (1959).

INFLUENCE OF EXCHANGE INTERACTION ON PARAMAGNETIC RELAXATION TIMES*

J. P. Goldsborough,† M. Mandel, and G. E. Pake
Department of Physics, Stanford University, Stanford, California
(Received November 12, 1959)

Previous investigations have shown that the spin-lattice relaxation time T_1 is equal to the inverse line width[1] T_2 and is independent of temperature in the range 77°K to room temperature in a crystalline free radical with a highly exchange-narrowed line.[2] We have found departures from this behavior in T_1 for several free radicals between 1.5°K and room temperature using the saturation technique.

The measurements were made at 10 kMc/sec and 24 kMc/sec with a conventional magic tee microwave bridge. The solid free radicals used were α,α-diphenyl β-picryl hydrazyl (DPPH), α,γ-bisdiphenylene β-phenyl allyl (BDPA), Wurster's blue perchlorate, and some solid solutions of DPPH in polystyrene. In all of these free radicals the exchange interaction between neighboring spins narrows the resonance line[3] in accordance with the approximate expression[4,5] $\Delta\omega \approx \omega_p^2/\omega_E$, where $\Delta\omega$ is the observed line width, ω_p is the dipolar frequency, and ω_E is the exchange frequency. From our observed line widths and calculations of the dipole width based on Van Vleck's second moment expression,[3] we estimate the exchange frequency to lie between 10 and 40 kMc/sec. In addition, we have investigated solid solutions of DPPH in polystyrene, where the exchange frequency varied from effectively zero to about 10 kMc/sec. DPPH samples recrystallized from different solvents were found to have different line widths as reported by Lothe and Eia.[6] This is because the solvent molecules influence the free radical spacing and thus the exchange interaction.

We have found that in DPPH, BDPA, and Wurster's blue the spin-lattice relaxation time T_1 is approximately equal to the spin-spin relaxation time T_2 at 77°K and room temperature. In those substances with higher exchange frequency as indicated by the narrower lines, T_1 is more nearly equal to T_2 and temperature independent. Table I shows these line widths and relaxation times.

The solid solutions were made by dissolving DPPH and polystyrene in chloroform and letting the chloroform evaporate. In the most concentrated solution T_1 was found to be equal to T_2 and temperature independent. As the concentration is reduced, T_1 becomes longer than T_2 and also shows a temperature dependence. When the concentration is reduced sufficiently, the exchange interaction diminishes and the hyperfine structure characteristic of DPPH appears. Upon further dilution the line width and shape remain the same, but T_1 continues to increase. Finally, T_1 becomes independent of concentration. Figure 1 is a plot of the above-described result.

These results can be interpreted using the three-reservoir model of Bloembergen and Wang,[2] which was discussed further by Van Vleck.[7] Figure 2 depicts schematically the thermodynamic reservoirs and the relaxation times. Since the exchange Hamiltonian $H_E = -\sum_{ij} J_{ij}\vec{S}_i\cdot\vec{S}_j$ commutes with the Zeeman Hamiltonian $H_Z = \sum_i g\beta H_z S_{zi}$, we can ascribe two temperatures to the spin system, θ_Z relating to the Zeeman system and θ_E

Table I. Line widths and relaxation times for free radicals at room temperature and 77°K.

	BDPA	DPPH No. 1 (chloroform)	DPPH No. 2 (benzene)	Wurster's blue
Line width (gauss between points of maximum slope)	0.6	0.8	2.8	2.9
T_2 (sec)	1.0×10^{-7}	8×10^{-8}	2.4×10^{-8}	2.3×10^{-8}
T_1 (sec)	1.1×10^{-7}	8×10^{-8}	5×10^{-8}	6×10^{-8}

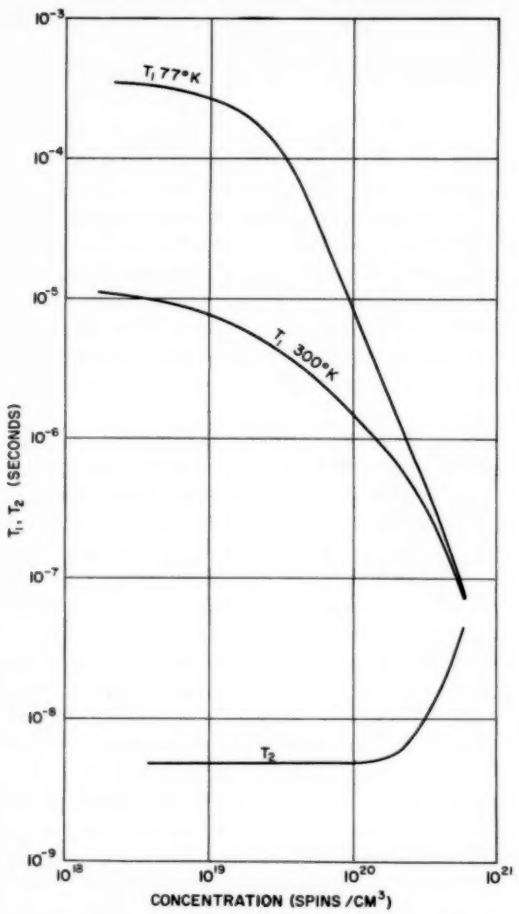

FIG. 1. Relaxation times of solid solutions of DPPH in polystyrene as a function of concentration. T_1 values are probably within a factor of two of the true value at low concentrations and 20% at the high concentrations. Ultimately both T_1 and T_2 would increase if higher concentrations were obtainable.

relating to the exchange energy. Both θ_Z and θ_E can be different from the lattice temperature θ_L. Energy transfer between the exchange system and the Zeeman system takes place because the exchange interaction randomly modulates the dipolar interaction. This may be illustrated by the similar random modulation of the dipolar interaction in liquids and the resultant motional narrowing, where the nonadiabatic part of the line width is approximately the relaxation time for energy exchange between the Zeeman system and the lattice.[5] Analogously, the nonadiabatic width for the exchange-narrowed resonance

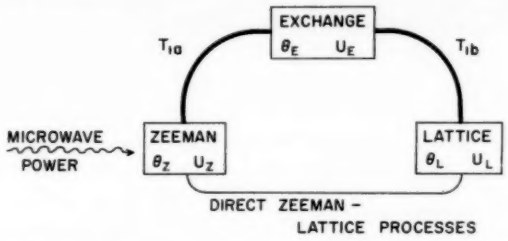

FIG. 2. Schematic diagram of the three-reservoir model of Bloembergen and Wang. The temperature θ and internal energy U of each reservoir is denoted by an appropriate subscript. The diagram also identifies the pairs of reservoirs coupled by the various relaxation times.

should represent the $1/T_1$ coupling the Zeeman and exchange systems. The Gaussian correlation spectrum usually employed, together with Eq. (36) of reference 5, gives an approximate form[8]

$$1/T_{1a} \approx (1/T_2)\exp(-\omega_Z^2/\omega_E^2). \quad (1)$$

Since this relaxation process does not involve the lattice phonons, it is independent of lattice temperature θ_L. The exchange-lattice relaxation time T_{1b} is due to the modulation of the exchange energy by the lattice vibrations and therefore should be strongly temperature dependent. The direct relaxation between the Zeeman system and the lattice is negligible.[7] In the region $k\theta_Z > 2\beta H$ and $k\theta_E > J$, the specific heats vary[9] as θ^{-2} and thus the Zeeman and exchange energies are $U_Z = -K_Z/\theta_Z$ and $U_E = -K_E/\theta_E$. If one defines T_1 as the inverse decay rate of internal energy, the following equations describe steady-state energy flow from left to right in Fig. 2 (ignoring direct processes):

$$\frac{dU_Z}{dt} = 0 = -\gamma^2 H_1^2 T_2 U_Z(\theta_Z) - \frac{1}{T_{1a}}[U_Z(\theta_Z) - U_Z(\theta_E)], \quad (2)$$

$$\frac{1}{T_{1a}}[U_Z(\theta_Z) - U_Z(\theta_E)] = \frac{1}{T_{1b}}[U_E(\theta_E) - U_E(\theta_L)]. \quad (3)$$

The observed ratio of Zeeman and lattice temperatures is interpreted as the saturation factor:

$$\theta_Z/\theta_L = 1 + \gamma^2 H_1^2 T_2 (T_1)_{\text{eff}}. \quad (4)$$

Equations (2), (3), and (4) yield

$$\theta_E/\theta_L = \frac{1 + \gamma^2 H_1^2 T_2 (T_1)_{\text{eff}}}{1 + \gamma^2 H_1^2 T_2 T_{1a}}, \quad (5)$$

where

$$(T_1)_{\text{eff}} = T_{1a} + (K_Z/K_E)T_{1b}. \quad (6)$$

Since the Zeeman and exchange energies are about the same order of magnitude, $K_Z/K_E \approx 1$ and therefore $(T_1)_{\text{eff}} \approx T_{1a} + T_{1b}$. In those samples with appreciable ω_E the observed $(T_1)_{\text{eff}}$ is temperature independent and equal to T_2. We conclude that $T_{1b} \ll T_{1a}$. In the solid solution samples of medium dilution, $(T_1)_{\text{eff}}$ is longer than T_2 in accord with Eq. (1), but only slightly temperature dependent, indicating that T_{1b} is still not long enough to be observed. With increasing dilution, exchange plays a smaller part in producing relaxation of the Zeeman system and finally the direct Zeeman-lattice relaxation is observed.

In the liquid helium temperature range we find a broadening of the lines in samples with a large exchange interaction. This is similar to the behavior observed in known antiferromagnetic substances as the Curie point is approached.[10] At room temperature the correlation frequency of the exchange system is approximately the exchange frequency $J/\hbar$. However, it may be that as the Curie point is approached the onset of local ordering reduces the correlation frequency. As the microwave power is increased, we observe a pronounced narrowing of the resonance line as well as a saturation of the total intensity. This effect is more pronounced in samples with higher exchange interaction. Effective spin-lattice relaxation times calculated from the saturation of total intensity (derivative peak×width^2) lie in the range of 10^{-6} sec and are temperature dependent. We believe that these relaxation times are determined by T_{1b}. This increase in relaxation time is too great to be explained by Eq. (1), even when the reduction of the correlation frequency is taken into account. Since T_{1a} is still about 5×10^{-8} sec, the temperature of the exchange system becomes greater than the lattice temperature upon saturation, in accord with Eq. (5). It is as if the increased exchange temperature destroys the local order thus raising the correlation frequency and narrowing the line.

In the samples with the highest exchange (DPPH-1, BDPA) we have observed a variation in line shape with power at temperatures below 2°K. In BDPA there is an increase in crystalline anisotropy below 2°K, since the observed line width of a polycrystalline sample is greater than that of a single crystal. In these cases the temperature may be below the Curie point. Specific heat measurements are in progress to determine the Curie temperatures in these materials.

We wish to thank Professor C. Kittel for communicating to us some of his ideas concerning exchange as a heat reservoir.

---

*Supported in part by the U. S. Air Force through the Air Force Office of Scientific Research.

†National Science Foundation Predoctoral Fellow.

[1]J. P. Lloyd and G. E. Pake, Phys. Rev. 92, 1576 (1953).

[2]N. Bloembergen and S. Wang, Phys. Rev. 93, 72 (1954).

[3]J. H. Van Vleck, Phys. Rev. 74, 1168 (1948).

[4]P. W. Anderson and P. R. Weiss, Revs. Modern Phys. 25, 269 (1953).

[5]R. Kubo and K. Tomita, Proceedings of the International Conference on Theoretical Physics, Kyoto and Tokyo, September, 1953 (Science Council of Japan, Tokyo, 1954), p. 779, and J. Phys. Soc. Japan, 9, 888 (1954).

[6]Johan J. Lothe and Gunnar Eia, Acta Chem. Scand. 12, 1535 (1958).

[7]J. H. Van Vleck, Suppl. Nuovo cimento 6, 1081 (1957).

[8]Strictly, spectral components at ω_Z and $2\omega_Z$ of a spectrum $\exp(-\omega^2/\omega_E^2)$ are required, but the single exponential of Eq. (1) represents the dependence on ω_Z adequately for our purposes.

[9]J. H. Van Vleck, J. Chem. Phys. 5, 320 (1937).

[10]L. R. Maxwell and T. R. McGuire, Revs. Modern Phys. 25, 279 (1953).

MAGNETOPLASMA REFLECTION IN SOLIDS*

Benjamin Lax and George B. Wright
Lincoln Laboratory, Massachusetts Institute of Technology, Lexington, Massachusetts
(Received November 9, 1959; revised manuscript received December 2, 1959)

The reflection edge at the plasma frequency ω_p, due to the dispersive properties of charge carriers in solids, is split and shifted in the presence of a magnetic field. This splitting has been observed in InSb and HgSe, and has been utilized to measure m^*, the effective mass of the electrons, directly.

For a spherical energy surface, it can be shown that the index of refraction n in a magnetic field for propagation vector $\vec{\gamma} \| \vec{H}$ is given by

$$n_{\pm}^2(H) = \epsilon[1 - \omega_p^2/\omega(\omega \pm \omega_c)], \tag{1}$$

and for $\vec{\gamma} \perp \vec{H}$

$$n_{\|}(H) = n(0) = \epsilon\left[1 - \frac{\omega_p^2}{\omega^2}\right], \quad (\vec{E} \| \vec{H}) \tag{2}$$

$$n_{\perp}(H) = \epsilon\left[1 - \frac{(\omega^2 - \omega_p^2)\omega_p^2}{(\omega^2 - \omega_p^2 - \omega_c^2)}\right], \quad (\vec{E} \perp \vec{H}) \tag{3}$$

where $\omega_p^2 = Ne^2/m^*\epsilon$, $\omega_c = eH/m^*c$, N is the carrier concentration, and ϵ is the dielectric constant. Losses have been neglected since $\omega\tau >> 1$. The reflection coefficient,

$$R = [(n-1)^2 + k^2]/[(n+1)^2 + k^2],$$

for the refractive indices of Eqs. (1), (2), and (3) is shown in Fig. 1 as a function of frequency. For $\vec{E} \| \vec{H}$, or for zero field, the reflectivity vanishes when $n = 1$, and is unity at $n = 0$, corresponding to frequencies $\omega = \omega_p(1 + \frac{1}{2}\delta)$ and $\omega = \omega_p$, respectively; where $\delta = 1/\epsilon$. Similarly, for the magnetoplasma at $n = 1$,

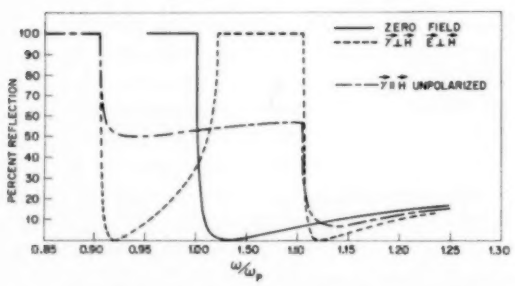

FIG. 1. Theoretical curves of magnetoplasma effect for isotropic carrier and $\omega >> 1$. $\omega_c = 0.2\omega_p$.

$$\omega_{\pm} \approx \omega_p(1 + \tfrac{1}{2}\delta) \pm \tfrac{1}{2}\omega_c - \tfrac{1}{8}\omega_c^2/\omega_p, \quad (\vec{\gamma} \| \vec{H}), \tag{4}$$

$$\omega_{\perp} \approx \omega_p(1 + \tfrac{1}{4}\delta) \pm \tfrac{1}{2}\omega_c + \tfrac{1}{8}\omega_c^2/\omega_p, \quad (\vec{\gamma} \perp \vec{H}), \tag{5}$$

where $\omega_p >> \omega_c$. There are two minima whose separation, $\Delta\omega$, is ω_c, for both longitudinal and transverse propagation. Consequently, this permits a direct determination of the effective mass of the electron. This technique may also be used to determine the electron concentration from the zero-field minimum, when ϵ is known. The analysis above may be generalized to a multiple carrier system, and to anisotropic energy surfaces.

The former is applicable to the type of valence band found in Ge and Si. For cubic crystals with ellipsoidal surfaces, the splitting, which is linear in H, is isotropic, and is given by

$$\Delta\omega = \omega_t(K+2)/(2K+1). \tag{6}$$

Here $K = m_l/m_t$; $\omega_t = eH/m_t c$; m_l and m_t are the longitudinal and transverse masses. The zero-field minimum for this case occurs at $\omega = \omega_p^*(1 + \frac{1}{2}\delta)$, where the effective mass in ω_p^* is $m^* = m_t 3K/(2K+1)$. If the carrier concentration and dielectric constant are known, then the mass parameters are determined by the zero-field minimum and the splitting.

The quadratic shift in a cubic crystal with ellipsoidal energy surfaces is not isotropic. For ellipsoids in Ge and Si, the shift, best observed for $E \| H$, can be shown to have the form[1]

$$\Delta\omega \approx (\omega_t^2/\omega_p)\,\frac{(K-1)^2}{rK(2K+1)}, \tag{7}$$

where $r = 3$, 9, and 6 for H parallel to the [001], [111], and [110] axes, respectively, in Ge, and $r = 3$ or 8 for H along the [111] or [110] axes in Si. $\Delta\omega = 0$ for $H \| [001]$ in Si. Similar results can be obtained for the quadratic shift when $E \perp H$, and these can be used to determine the orientation of the surfaces and the mass parameters. For warped surfaces, as for the heavy hole in Ge and Si, the anisotropy of the quadratic shift can also be evaluated.[2]

It can be shown that in the low-field limit ($\omega_c < \omega_p$), if the current is expressed as a power series in H, then magnetoplasma phenomena are

the dispersive analogs of the galvanomagnetic effects. Writing[3]

$$J_i = \sigma_0 E_i + \sigma_{ij} E_i H_j + \sigma_{ijk} E_i H_j H_k + \ldots, \qquad (8)$$

we derive the plasma frequency from σ_0, the linear splitting from σ_{ij}, and the quadratic shift from σ_{ijk}. These dispersive phenomena are seen to correspond, respectively, to the conductivity σ_0, Hall coefficient σ_{ij}, and magnetoconductivity coefficient σ_{ijk}, of the dissipative galvanomagnetic phenomena. The latter measure τ/m^*, while the former measure m^* directly.

The other limit of the magnetoplasma effect, i.e., $\omega_c > \omega_p$, has been considered in connection with cyclotron resonance.[4,5] However, the experiments have been performed with the magnetic field as the variable. If instead, the frequency is varied, then from Eqs. (1) and (3) two minima of the reflection occur near $\omega \approx \omega_c + \omega_p^2/\omega_c$ and $\omega \approx \omega_p^2/\omega_c$. The first represents the magnetoplasma shift of the cyclotron resonance, and the second the "magnetoplasma resonance" of Dresselhaus, Kip, and Kittel.[4] Phenomena similar to the effects discussed here have been observed in bismuth, where the anisotropy of the plasma edge is provided by the crystal itself.[5]

The experimental results for a sample of InSb with a carrier concentration of 1.8×10^{18} cm^{-3}, as determined by Hall measurements, are shown in Fig. 2. The zero-field reflection curve agrees with those of Spitzer and Fan[6] for a similar carrier concentration. With the application of a magnetic field, two distinct minima appear, whose separation increases linearly with magnetic field. The shape of the curves differs somewhat from the theoretical curves of Fig. 1 in that the peak between the minima does not go to 100% reflection, nor do the minima go to zero, even at high fields. We believe that these differences may be attributed to the neglect in the theory of the effects of scattering and of the statistical distribution of the electrons over the energy band at room temperature.

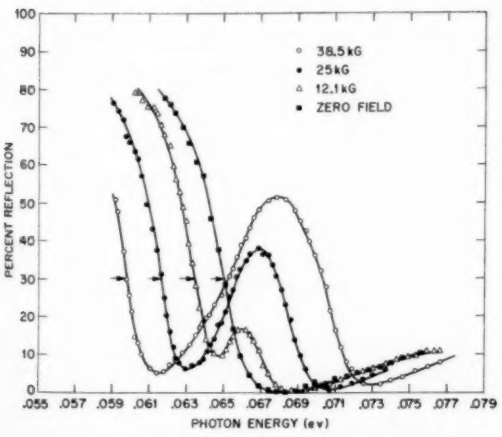

FIG. 2. Magnetoplasma effect in n-type InSb. $N = 1.8\times10^{18}$ cm^{-3}.

Although it is possible to obtain the effective mass from the separation of the minima, better resolution is obtained by plotting the shift of the plasma edge at an isoreflection point, as shown by the arrows in Fig. 2. This shift as a function of magnetic field is shown in Fig. 3. The variation is linear, in accordance with the theory. The value of the effective mass obtained from the slope of this line for InSb is $m^*/m_0 = 0.041 \pm 0.002$. Using the method of Spitzer and Fan,[6]

$$\frac{m^*}{m_0} = \frac{N\lambda_{\min}^2}{(\epsilon - 1)} \times 8.97\times10^{-22}, \qquad (9)$$

with $N = 1.8\times10^{18}$ from Hall measurements, $\lambda_{\min} = 18.3\ \mu$ the wavelength of the zero-field minimum, and $\epsilon = 14.9$ the dielectric constant at 18.3 μ,[7] we obtain a mass $m^*/m_0 = 0.039 \pm 0.004$. We see that the agreement is within experimental error.

From curves for HgSe similar to those of

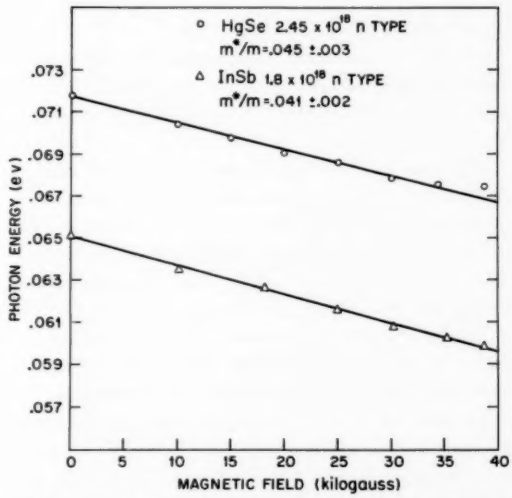

FIG. 3. Shift of the plasma edge for 30% reflection point as a function of magnetic field for n-type InSb and HgSe.

Fig. 2, we obtain the shift of the plasma edge shown in Fig. 3. Analysis of these data gives a mass of $m^*/m_0 = 0.045 \pm 0.003$ for an electron concentration of 2.45×10^{18} cm^{-3}. The zero-field technique for determining the effective mass could not be applied to this material, because the dielectric constant was not known, and was very difficult to measure directly. In this case, therefore, we may invert the method of Spitzer and Fan, and by using the value of effective mass determined from the magnetoplasma effect, find the dielectric constant $\epsilon = 14.0$ at 16.3 microns.

These experiments can be extended over a frequency range from millimeter waves to the ultraviolet to determine band structure constants not accessible by other techniques. With the availability of high magnetic fields, of the order of 100 kilogauss or more, the important classes of materials which may be studied over a wide range of temperature include metals and semimetals, materials of high effective mass, and semiconductors with a wide range of carrier concentration.

It is a pleasure to acknowledge the help of Dr. T. C. Harman, who supplied the HgSe samples and Hall measurements, and Dr. A. J. Strauss, who supplied the InSb. The authors are grateful for stimulating discussions with Mr. Richard N. Brown and Dr. John G. Mavroides. Mrs. M. Lavine developed the etch for the HgSe, Mr. C. A. Lewis prepared the samples, and Mr. J. R. Williamson helped with data taking.

---

*Work performed with the joint support of the U. S. Army, Navy, and Air Force.

[1]B. Lax and L. Roth, Phys. Rev. 98, 548 (1955).

[2]B. Lax and J. G. Mavroides, Phys. Rev. 100, 1650 (1955); J. G. Mavroides and B. Lax, Phys. Rev. 107, 1530 (1957).

[3]S. Meiboom and B. Abeles, Phys. Rev. 93, 1121 (1954); B. Abeles and S. Meiboom, Phys. Rev. 95, 31 (1954).

[4]Dresselhaus, Kip, and Kittel, Phys. Rev. 100, 618 (1955).

[5]Boyle, Brailsford, and Galt, Phys. Rev. 109, 1396 (1958).

[6]W. G. Spitzer and H. Y. Fan, Phys. Rev. 106, 882 (1955).

[7]Moss, Smith, and Hawkins, Proc. Phys. Soc. (London) B70, 776 (1957).

SPIN-LATTICE RELAXATION TIMES IN RUBY AT 34.6 kMc/sec

J. H. Pace, D. F. Sampson, and J. S. Thorp
Physics Department, Royal Radar Establishment, Great Malvern, England
(Received November 19, 1959)

The factors governing spin-lattice relaxation processes are not completely clear and the results of measurements which have previously been made[1-3] in the 7-9 kMc/sec region and at 24 kMc/sec suggest that existing theory[4] may not be adequate. Some measurements of spin-lattice relaxation time have therefore been made in ruby at 34.6 kMc/sec between 1.4°K and 90°K; the polar angle used was $\theta = 90°$, and the concentration chosen was 0.1% Cr (nominal) since this has been widely used in masers. The relaxation times for the $\Delta 1$ transitions are of the same order of magnitude as at lower frequencies. For the $\Delta 2$ and $\Delta 3$ transitions, however, appreciably different times were observed at 1.4°K, though the relaxation times for all transitions approach a common value at about 77°K. These results enable some deductions to be made regarding relaxation processes. They also indicate that ruby is a promising material for extending maser techniques to the millimeter region.

A pulse saturation method[5] was used in which the transition studied was saturated by a short pulse, recovery to thermal equilibrium being observed by measuring the absorption of a low-power cw monitoring signal of the same frequency. The maximum pulse power available was 6 watts (peak), and the monitoring signal level was about 2 μw. The pulse length used was 200 μsec with a repetition rate of up to 25 cps; under these conditions the minimum pulse power required for saturation was 60 mw at 1.4°K. The low-temperature assembly was a straight cupro-nickel waveguide (inside dimensions 0.280 in. × 0.140 in.), terminated by a removable plane plunger. The specimen, an exact fit in the guide, was mounted on the plunger; its volume was 0.2 cc and the chromium concentra-

tion nominally 0.1%. The crystal c axis was oriented perpendicular to the dc magnetic field to obtain a simple energy level diagram minimizing the possibility of cross-relaxation effects.[1] The over-all accuracy of the measurements was estimated to be within ±10%; the minimum measurable relaxation time was set by the receiver recovery time, which was 5 μsec.

Analysis of the recovery curves showed them to be substantially single exponentials, enabling a unique value to be given to the spin-lattice relaxation time. For the +3/2 to +1/2, (Δ1), transition the values obtained at different temperatures for $\theta = 90°$ were:

Temperature (°K)	T_1 (milliseconds)
1.4	59
4.2	22.5
10.1	10.0
20.3	6.0
57	0.10
77	0.044
90	0.017

As far as comparison with previous measurements on different ruby samples can be made, these values are of the same order as those reported at 7.2 kMc/sec,[1] 9.3 kMc/sec,[2] and 24.2 kMc/sec.[3] It appears therefore that over this range T_1 does not vary appreciably with frequency. No general theoretical rule for the frequency dependence can be made, since this is determined by both the material and the coupling mechanism; it may be noted, however, that a variation as frequency^{-2} or frequency^{-4}, predicted by Van Vleck[4] for chrome alum, is not found.

In the helium/hydrogen range the relaxation time is approximately inversely proportional to temperature; this behavior is similar to that at 9.3 kMc/sec.[2] Preliminary results show that this relation breaks down between 20°K and 57°K, and that above 57°K the decrease in relaxation time with increasing temperature is much more rapid, though not so great as (temperature)$^{-7}$; see Van Vleck.[4]

Relaxation times for other transitions were also measured at $\theta = 90°$. At 1.4°K the values are appreciably different:

Transition	T_1 (milliseconds)
$+\frac{1}{2}$ to $-\frac{1}{2}$ (Δ1)	64
$(+\frac{3}{2}$ to $+\frac{1}{2})$(Δ1)	59
$+\frac{1}{2}$ to $-\frac{3}{2}$ (Δ2)	147
$+\frac{3}{2}$ to $-\frac{1}{2}$ (Δ2)	100
$+\frac{3}{2}$ to $-\frac{3}{2}$ (Δ3)	296

These differences lie well outside experimental error, and it thus appears that it is not valid to assume a single relaxation time for all levels. At higher temperatures the differences are reduced, and initial measurements suggest that the relaxation time for all these levels approaches a common value at about 77°K.

This paper is published by permission of the Controller, H.M.S.O.

---

[1]W. B. Mims, Radio-Frequency Spectroscopy Conference, Oxford, 1959 (unpublished).

[2]A. F. Harvey and J. C. Gill, Royal Radar Establishment, Malvern (unpublished).

[3]Kikuchi, Lambe, Makhov, and Terhune, J. Appl. Phys. 30, 1061 (1959).

[4]J. H. Van Vleck, Phys. Rev. 57, 426 (1940).

[5]Davis, Strandberg, and Kyhl, Phys. Rev. 111, 1268 (1958).

INFLUENCE OF DEGENERACY ON RECOMBINATION RADIATION IN GERMANIUM

J. I. Pankove
RCA Laboratories, Princeton, New Jersey
(Received November 20, 1959)

A tunnel diode[1] was fabricated by successive recrystallizations of n- and p-type germanium from solution in, respectively, donor- and acceptor-rich alloys. The diode formed a small area (about 10 mils in diameter) on a Weierstrass sphere[2] of purer germanium. This structure concentrates the radiation and free carrier absorption is negligible. The specimen is mounted at the bottom of a Dewar forming simultaneously a source of radiation, a lens, and a window.

The diode was pulsed in the forward direction at 13 cps with 50% duty-cycle square waves. The measurements were made at 77°K. From the V-I characteristic it is evident that the emission here reported was obtained while the diode was biased in the injection mode.

The emission spectrum is shown in Fig. 1 as a family of curves with current as the parameter. One notes the presence of two peaks: a low-energy peak which moves to higher energies as the current increases and a rapidly growing peak at 0.71 ev. The low-energy tail of the spectrum saturates; the growths of the low-energy peak and of the 0.71-ev peak are shown in Fig. 2.

It is believed, tentatively, that this spectrum represents the occupancy of the degenerate conduction band. According to this hypothesis, the intrinsic conduction band would be degenerated by the presence of a broad impurity band (Fig. 3). This model is reminiscent of the "tailing-off" of the density-of-states curve predicted for disordered alloys.[3] At equilibrium, the impurity band is only partially filled. For a small injection, radiative transitions from all the occupied states take place and their spectrum would describe approximately the occupancy of the impurity band, allowing for some broadening due to a small spread of states available in the valence band (those occupied by injected holes). At higher currents, the Fermi level (a) would rise in the degenerate conduction band. The new

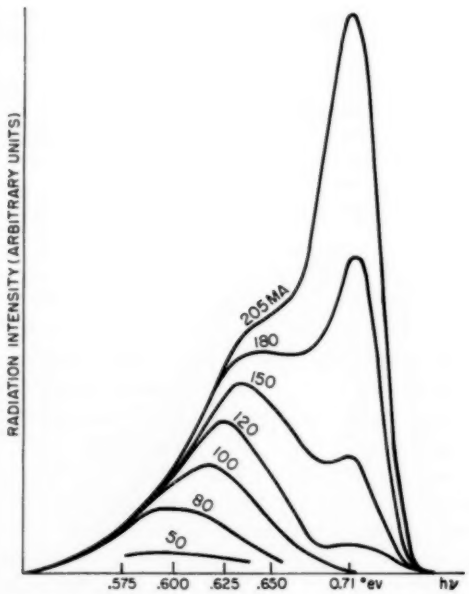

FIG. 1. Emission spectrum from tunnel diode.

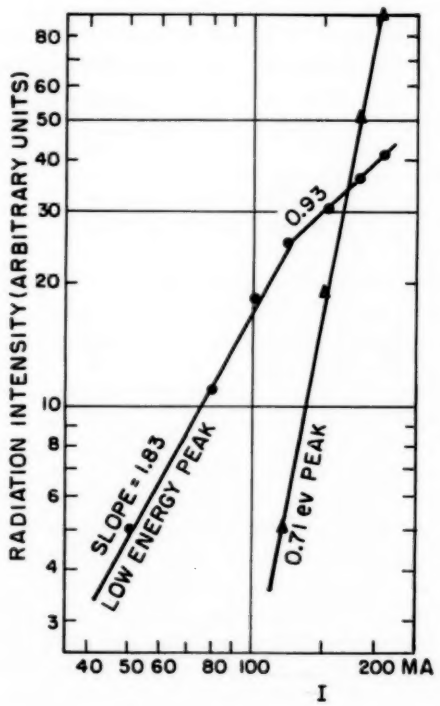

FIG. 2. Current dependence of two emission peaks.

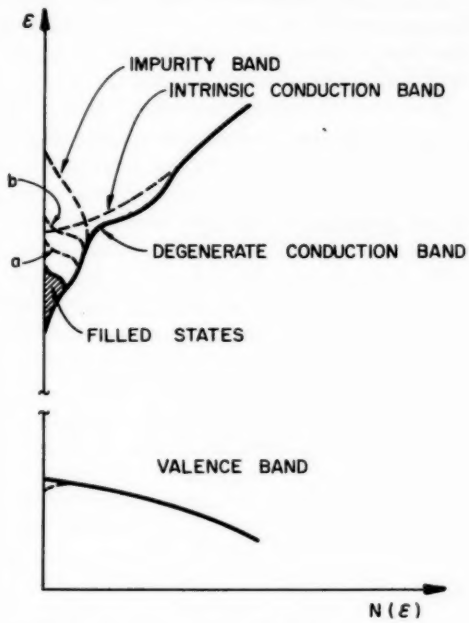

FIG. 3. Diagram for density of states and their occupancy.

fully occupied levels represent excess carriers which recombine through a bimolecular process. This model agrees with the shift of the radiation peak and with its rate of growth. Once a conduction-band state is fully occupied, the number of transitions from that state to the valence-band states which are saturated with holes cannot increase any further. This would explain the saturation of the low-energy tail. The linear rise of radiation with current would correspond to transitions from saturated states in the degenerate conduction band to nonsaturated states in the valence band. The sharp rise of the 0.71-ev peak would correspond to the exponential growth of the population of states in the intrinsic conduction band while the latter is penetrated by the Boltzmann tail (b) of the Fermi distribution.

The shift of the low-energy peak implies that at equilibrium the Fermi level is about 0.1 ev below the intrinsic conduction band. It is estimated that only a fraction of the order of 10^{-4} of the input power is emitted in the reported spectrum.

The author is grateful for discussions with Professor Aigrain who stimulated the interest in this experiment. Thanks are also due to E. F. Davison who artfully fabricated the specimen.

[1]L. Esaki, Phys. Rev. 109, 603 (1958).
[2]P. Aigrain and C. Benoit à la Guillaume, J. phys. radium 17, 709 (1956).
[3]R. H. Parmenter, Phys. Rev. 97, 587 (1955).

MECHANISM OF TRANSFER REACTIONS WITH HEAVY IONS

A. Zucker
Oak Ridge National Laboratory,* Oak Ridge, Tennessee
(Received December 4, 1959)

Heavy-ion nuclear reactions in which only a small portion of the nuclear matter is transferred from one nucleus to the other, presumably without the formation of a compound system, are generally called transfer reactions. The simplest transfer reaction involves the transfer of a nucleon, from one nucleus to the other. It was found[1] that neutron transfer reactions are strongly Q-dependent and that their cross sections increase with energy rather slowly once a critical energy $E^* = E_{c.m.} - E_{barr} + \frac{1}{2}Q$ is reached. At the low energies available in this laboratory, 28-Mev N^{14}, neutron transfer reaction cross sections are at most ~5 mb. The measurements of Volkov, Pasiuk, and Fliorov[2] show that the neutron transfer cross sections for N on Al and Ni level off, the former around 10 mb and the latter around 30. These measurements were made for energies up to 105 Mev. Volkov et al. also estimate that the proton transfer cross sections have the same energy dependence and are about 40% of the neutron transfer cross section in Al and 17% in Ni.

Two-neutron transfer reactions, in which two neutrons are attached to the incident N^{14}, thus forming radioactive N^{16}, were observed by Karnaukhov, Ter-Akopian, and Khalizov.[3] They estimate the cross section on Cu to be ~0.15 mb

for an integrated energy spectrum from 92 to 55 Mev, and ten times smaller on Al.

Recently two new independent observations have been made which deal with the general question of transfer reactions. The first is by Anderson, Knox, Quinton, and Bach[4] who with the use of counters observed that large numbers of oxygen, nitrogen, carbon, boron, and even lithium ions are produced from the 160-Mev oxygen bombardment of aluminum. The energy distribution of these particles is quite broad and they seem to be preferentially emitted in the forward direction. Relatively few ions heavier than oxygen, such as fluorine and neon, are observed. Second, Kaufmann and Wolfgang[5] bombarded Al, Cu, and Sn with 140-Mev nitrogen and 160-Mev oxygen ions. They found that O^{15}, N^{13}, and C^{11} are produced in all their experiments. While the appearance of O^{15} and N^{13} from the nitrogen bombardments can be readily interpreted as due to nucleon transfer, the production of C^{11} is interpreted by the authors as a $(p2n)$ transfer. In the oxygen bombardments the production of N^{13} and C^{11} is similarly interpreted as a $(p2n)$ transfer and a $(2p3n)$ transfer. The authors further state that it seems plausible that the $(p2n)$ transfer involves the exchange of a proton and an α particle, while the $(2p3n)$ transfer is a double transfer of an α particle and a neutron. Here we use the terms exchange transfer to mean the simultaneous transfer of an entity from each of the participating nuclei to the other, and double transfer as the transfer of two entities from one nucleus to the other.

The cross sections measured by Kaufmann and Wolfgang for the $(p2n)$ and $(2p3n)$ transfers are of the order of a few millibarns. This is a surprisingly large number in view of the fact that the $(2n)$ double-transfer cross sections measured by Karnaukhov and co-workers are one or two orders of magnitude smaller. The exchange transfer mechanism does not seem to be a very probable one either. Pinajian[6] has measured the cross section for a (p,n) exchange for nitrogen on aluminum to be about 2 μb at 27 Mev. A classical calculation by Goldansky[7] predicts that the (n,n) exchange transfer near the barrier should have a cross section in the region of 1-10 μb.

In the cases where Kaufmann and Wolfgang interpret the production of C^{11} and N^{13} as resulting from $(2p3n)$ and $(p2n)$ transfers it appears worthwhile to consider the possibility of single nucleon transfers and subsequent de-excitation in a two-step reaction, as an alternative or at least supplementary explanation. For example $O^{16}+\mathrm{Sn}\rightarrow O^{15*}+\mathrm{Sn}$, followed by $O^{15*}\rightarrow C^{11}+\alpha$. The threshold for this process requires that O^{15} be excited to 10.2 Mev plus a little more for the α particle to overcome the Coulomb barrier. The competing de-excitation processes have a threshold at 13.2 Mev for neutron de-excitation and at 7.30 Mev for proton de-excitation. Thus, although proton de-excitation is favored, O^{15} formed at 15-Mev excitation and higher will result in appreciable amounts of C^{11}. It has been shown by Halbert and Zucker[8] that in the reaction $Mg^{25}(N^{14},N^{13})Mg^{26}$ excited states in Mg^{26} as high as 7 Mev occur at an incident energy of 27.2 Mev. There appears to be no reason why much higher excited states cannot be populated in a nucleon transfer reaction at higher incident energies. The presence of N^{13} in oxygen-induced reactions can be explained by a proton transfer and alpha de-excitation: $O^{16}+\mathrm{Sn}\rightarrow F^{17*}+\mathrm{In}$, $F^{17*}\rightarrow N^{13}+\alpha$. The threshold for this reaction is 5.80-Mev excitation in F^{17}. N^{13} can also be produced by $O^{16}+\mathrm{Sn}\rightarrow O^{15*}+\mathrm{Sn}$, $O^{15*}\rightarrow N^{13}+p+n$, although the threshold is now 17.85 Mev. Finally C^{11} can be produced in N^{14}-induced reactions by $N^{14}+\mathrm{Sn}\rightarrow O^{15*}+\mathrm{In}$, $O^{15*}\rightarrow C^{11}+\alpha$, or by p or n transfer to C^{13*} or N^{13*} and de-excitation by the emission of (pn) or $(2n)$. The single transfer and subsequent de-excitation process does not necessarily exclude the contact transfer mechanism proposed by Kaufmann and Wolfgang. Both may in fact be operative in the production of the nuclides observed.

It is not necessary that the reactions outlined above proceed in the order indicated. They may in fact occur simultaneously as three-body disintegrations, i.e., $O^{16}+\mathrm{Sn}\rightarrow \mathrm{Sn}+C^{11}+\alpha$.

If transfers of entities such as α particles or deuterons turn out to have high cross sections they would also contribute to the observed yields by the de-excitation of residual nuclei.

Two features of Kaufmann and Wolfgang's data support the de-excitation mechanism. The spread in range of both N^{13} and C^{11} from $O^{16}+\mathrm{Sn}$ is twice as great as the spread of the O^{15}, which may be due to the recoil of the α particle. The recoil not only changes the energy but also changes the direction of the N^{13} or C^{11}, thus smearing out the range in two ways. The ratio of the cross sections of $(p2n)$ transfers to (n) transfers and $(2p3n)$ to (n) transfers is the same for the three targets studied. This would be expected for the mechanism proposed here.

The transfer and de-excitation process can

also be applied to the results of Anderson, Knox, Quinton, and Bach. The broad energy distribution of heavy fragments may be due to the population of excited states in the residual nuclei. The lack of F, Ne, and heavier fragments follows from the de-excitation picture also. It would otherwise be quite puzzling why transfers from O^{16} to Al^{27} are so probable while transfers the other way are rarer by an order of magnitude, especially in view of the tightly bound structure of oxygen.

It is not the purpose of this paper to demonstrate that complex transfers such as $(p2n)$ or $(2p3n)$ do not occur, but rather that the existing data can be explained by simpler transfers and subsequent de-excitation of residual nuclei. In any event this mechanism should be considered in the interpretation of heavy-ion reactions.

The author is indebted to Dr. Knox, Dr. Quinton, Dr. Anderson, and Dr. Bach, who graciously allowed him the use of their data before publication, and to Dr. Halbert and Dr. Pinajian for instructive discussions.

*Operated for the U. S. Atomic Energy Commission by Union Carbide Corporation.

[1]Fisher, Zucker, and Gropp, Phys. Rev. 113, 542 (1959).

[2]Volkov, Pasiuk, and Fliorov, Zhur. Eksptl. i Teoret. Fiz. 33, 595 (1957) [translation: Soviet Phys. JETP 6, 459 (1958)].

[3]Karnaukhov, Ter-Akopian and Khalizov, Zhur. Eksptl. i Teoret. Fiz. 36, 748 (1959)[translation: Soviet Phys. JETP 9, 525 (1959)].

[4]Anderson, Knox, Quinton, and Bach (private communication).

[5]R. Kaufmann and R. Wolfgang, Phys. Rev. Letters 3, 232 (1959).

[6]J. J. Pinajian, Bull. Am. Phys. Soc. 4, 219 (1959).

[7]V. I. Goldansky, Nuclear Phys. 9, 551 (1958).

[8]M. L. Halbert and A. Zucker, Phys. Rev. 108, 336 (1957).

BETA-ALPHA ANGULAR CORRELATIONS IN B^8 AND Li^8†

M. E. Nordberg, B. Povh,* and C. A. Barnes
Kellogg Radiation Laboratory, California Institute of Technology, Pasadena, California
(Received December 10, 1959)

It has been suggested by Bernstein and Lewis[1] that a comparison of the β-α angular correlations in the isotopic spin triplet of mass 8 (Li^8, Be^8, B^8) might lead to a test of the conserved vector current theory of β decay.[2] These authors assumed $\Gamma(M1) = 0.15\ \Gamma_W$, where Γ_W is the Weisskopf unit, as a probable width for the $M1$ decay of the $J=2^+$, $T=1$ Be^8 state (analog state of the Li^8 ground state) to the $J=2^+$, $T=0$ state of Be^8. Taking the observed[3] near-isotropy of the β-α angular correlation in Li^8 as indicating the near cancellation of the various possible forbidden corrections to the predominantly allowed Li^8 β transition,[4] Bernstein and Lewis predicted a β-α angular correlation in B^8 as follows:

$$W(\theta) \approx 1 \pm 0.1 P_2(\cos\theta) \approx 1 \pm 0.15\cos^2\theta.$$

We have measured the β-α angular correlations in Li^8 and in B^8 and have found that the difference in the angular correlations is probably not greater than 1/4 of the predicted difference.

In the present experiment Li^8 was produced by bombarding thin targets of natural lithium with 0.75-Mev deuterons, and B^8 was produced by bombarding thin targets of enriched Li^6 (99.7% Li^6) with He^3 ions of 3.15 Mev. The bombarding beams were allowed to strike the target for 0.4 second and then interrupted by a mechanical chopper. After a delay of 0.1 second the electronic circuits were switched on for 0.4 second. The cycle repeated after a further delay of 0.1 second.

The β rays were detected in a 3-in. deep plastic scintillator, which could be rotated around the target axis between 90° and 180° with respect to a fixed, silicon surface-barrier, α detector. A "slow-fast" coincidence system was used with a time resolution of 35 mμsec for the Li^8 experiment, and 80 mμsec for the B^8 measurements. The random to real coincidence ratios were, respectively, 0.06 and < 0.01 for the Li^8 and B^8 runs. Pulses from the α detector were displayed on a 100-channel analyzer, when a fast coincidence was recorded during the proper counting part of the cycle, and when the β-ray pulse lay between limits selected by a single-channel analyzer.

The coincident α spectrum was displayed in this way, in order to evaluate the energy loss of the α particles in escaping from the target. This

information is necessary, since the α particles coincident with 180° β rays are shifted upwards in energy by recoil from the β rays and neutrinos, and this energy shift makes the laboratory solid angle of the α counter larger than the center-of-mass solid angle by an amount which depends on the β-ray energy, and original energy of the α particle in the center-of-mass system. For $E_\alpha \approx 1.5$ Mev, and $E_\beta > 9.7$ Mev, this solid angle correction is $\approx 10\%$. The ratio of solid angles is

$$\Omega_{\text{c.m.}}/\Omega_{\text{lab}} \approx 1 - 2V_{\text{recoil}}/V_\alpha$$
$$\approx 1 - (\overline{E}_\beta - \tfrac{1}{3}\overline{E}_\nu)/86.4(E_\alpha)^{1/2},$$

where we have assumed the axial-vector β interaction,[4] and the energies are in Mev. It should be noted that the solid angle corrections are similar in the Li^8 and B^8 runs, so inaccuracies in making these corrections tend to cancel in the ratio of the two angular correlations. The coincident α spectra are shown in Figs. 1 and 2. The singles (noncoincident) α-particle, and β-ray counts were recorded at the two angles of the β-ray counter and used to correct the ratio of coincident counts at 180° to the coincident counts at 90°. In the Li^8 runs the target surface was at 45° with respect to the incident beam as in Fig. 1. This meant that absorption in the 2-mil aluminum target backing was the same for both positions of the β counter. Under these conditions the corrections made to the coincidence ratio for inequalities in the singles rates were $< 1.5\%$.

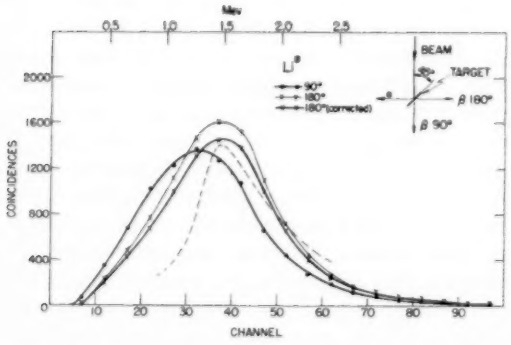

FIG. 1. α spectra in coincidence with β rays at 90° and 180° in the β decay of Li^8. The curve marked 180° (corrected) has been corrected for solid angle effects as discussed in the text. The dashed curve is the thin-target α spectrum obtained by R. T. Frost and S. S. Hanna, Phys. Rev. 99, 8 (1955), for comparison purposes.

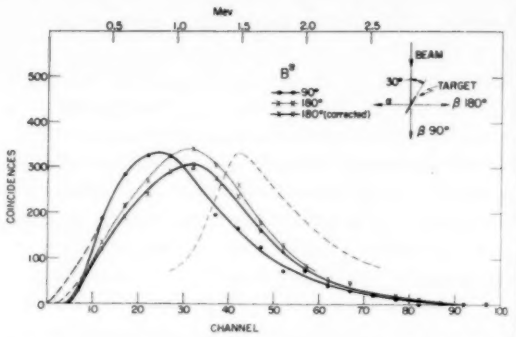

FIG. 2. α spectra in coincidence with β rays at 90° and 180° in the β decay of B^8. The dashed extrapolations to zero pulse size, represent a possible correction for coincidence inefficiency below channel 10, as described in the text.

The higher compound nucleus recoil velocity in the $Li^6(He^3,n)B^8$ reaction at 3.15 Mev caused the α particles to lose an excessive amount of energy in escaping from the target, when the target was placed at 45° to the beam direction. With the target plane at an angle of 20° to the beam, the singles rates gave a 6% correction to the coincidence rates, while a target angle of 30° to the beam gave a singles correction $< 3\%$. There is also a possibility that inefficiencies in the electronic circuits were causing a loss of α particles from the spectra below channel 10. This alters the 90° spectrum more than the 180° spectrum because of the energy shift of the 180° spectrum due to recoil from the β rays. The dashed extrapolations shown in Fig. 2 probably represent better estimates of the α spectra.

The results are summarized in Table I where the errors quoted are statistical only.

If the results of Hanna et al.[3] are corrected for solid angle on the basis of the axial vector interaction, rather than on the basis of the tensor interaction, then believed correct, they yield $W(\theta) \approx 1 + 0.03(\pm 0.03)\cos^2\theta$ for Li^8 in close agreement with the present work.

The present results suggest that the ratio, $(I_{180°}/I_{90°})_{Li^8}/(I_{180°}/I_{90°})_{B^8}$, is 1.02 ± 0.04, where the error quoted is statistical only, to be compared with the predicted value, 1.15 or 0.85. The failure to observe the expected large asymmetry could be due either to the failure of the conserved vector current theory, or to an unusually small $M1$ matrix element. Experimental and theoretical attempts to estimate the $M1$ matrix element are in progress. If it is the case

Table I. Summary of measured asymmetries in the β-α angular correlations of Li^8 and B^8.

β decay and E_β	Target angle to beam	Corrected $I_{180°}/I_{90°}$
Li^8, $E_\beta > 9.7$ Mev	45°	1.03 ± 0.02
Li^8, 3.8 Mev $< E_\beta < 6.1$ Mev	45°	1.03 ± 0.02
Li^8, $1.5 < E_\beta < 3.8$ Mev	45°	1.05 ± 0.02
B^8, $E_\beta > 9.7$ Mev	30°	1.02 ± 0.03
B^8, $E_\beta > 9.7$ Mev	20°	1.00 ± 0.05
B^8, $E_\beta > 9.7$ Mev	30°	1.00 ± 0.03[a]

[a] Using the dashed extrapolations in Fig. 2.

that the $M1$ matrix element is anomalously small, then the present experiment would not be a suitable method for testing the conserved vector current hypothesis, since there are probably other corrections of the order of a few percent which could mask the expected anisotropy,[5] for example, a term proportional to the $E2$ matrix element.

The authors would like to acknowledge their indebtedness to Professor W. A. Fowler, Professor T. Lauritsen, and Dr. H. Weidenmuller for their advice and interest in this experiment.

†Supported in part by the joint program of the Office of Naval Research and the U. S. Atomic Energy Commission.

*Present address: The Institute "J. Stefan," Ljubljana, Yugoslavia.

[1]J. Bernstein and R. R. Lewis, Phys. Rev. 112, 232 (1958).

[2]R. P. Feynman and M. Gell-Mann, Phys. Rev. 109, 193 (1958); M. Gell-Mann, Phys. Rev. 111, 362 (1958); E. C. G. Sudarshan and R. E. Marshak, Phys. Rev. 109, 1860 (1958); S. S. Gershtein and J. B. Zeldovich, Zhur. Eksptl. i Teoret. Fiz. 29, 698 (1955) [translation: Soviet Phys. JETP 2, 576 (1957)].

[3]Hanna, LaVier, and Class, Phys. Rev. 95, 110 (1954); D. StP. Bunbury, Phys. Rev. 90, 110 (1953).

[4]Lauritsen, Barnes, Fowler, and Lauritsen, Phys. Rev. Letters 1, 326 (1958); Barnes, Fowler, Greenstein, Lauritsen, and Nordberg, Phys. Rev. Letters 1, 328 (1958).

[5]M. Morita, Phys. Rev. 113, 1584 (1959).

DECAY OF OXYGEN 20†

Gertrude Scharff-Goldhaber
Brookhaven National Laboratory, Upton, New York

and

Albert Goodman and Myron G. Silbert
Los Alamos Scientific Laboratory, Los Alamos, New Mexico

(Received December 2, 1959)

It is of considerable theoretical interest to discover the decay of the isotope O^{20} and its properties. Jarmie and Silbert,[1] by studying the energies of the protons produced in the reaction $O^{18}(t,p)O^{20}$, were able to deduce for the energy difference $Q(O^{20}-F^{20}) = 3.75$ Mev. However, earlier attempts[2-4] to search for the decay of the isotope have been unsuccessful. Katcoff and Hudis[3] were able to exclude a half-life of $10 \text{ min} \leq \tau_{1/2}(O^{20}) \leq 150$ yr with reasonable certainty, and Amiel and Segel[4] showed that $\tau_{1/2} \leq 30$ to 50 sec.

We studied the decay of O^{20} produced by 2.66-Mev tritons from the 3-Mev Los Alamos Van de Graaff in an O^{18} (95% enriched) gas target. As detector for the γ rays we used a scintillation spectrometer. The front face of a 3 in. × 3 in. NaI(Tl) crystal was placed about 4 in. from the

target, behind a $\frac{3}{8}$-inch Be absorber which removed β rays. A one-hundred channel pulse-height analyzer served to study the spectrum. Bombardments of one to five seconds duration were used. The spectra obtained during 10-sec counts, starting at various intervals (1-40 sec) after bombardment, were printed out. In addition to the 1.63-Mev line from F^{20}, which is the daughter product of O^{20} and also independently produced in the reaction $O^{18}(t,n)F^{20}$, we observed a weaker γ ray (~6% of the 1.63-Mev line) at 1.067 ± 0.020 Mev (Fig. 1, curve *A*). This energy agrees within limits of error with that of the fourth excited state[5] of F^{20} (1.059 ± 0.008 Mev), found in the reaction $F^{19}(d,p)F^{20}$. The decay curves of both the 1.63-Mev and the 1.067-Mev γ rays were followed by taking 1-sec counts obtained within a channel set at the appropriate energy. It was observed that both γ rays decay with half-lives of ~12.5 sec, which is in fair agreement with the 11.4-sec half-life reported[5] for F^{20}. The 1.06-Mev photopeak, of course, is superimposed on the Compton spectrum of the 1.63-Mev γ ray. The latter accounts for about 60-70% of the counts in the channel.[6]

We now made the tentative assumption that the beta decay of O^{20} takes place mainly to the 1.06-Mev state in F^{20} and that the half-life of O^{20} differs only slightly from that of F^{20}. To prove this we decided to measure the half-life and gamma-ray spectrum of F^{20} in the absence of O^{20}. For this purpose F^{20} was produced by bombarding F^{19} (CaF_2 crystal) with 2-Mev deuterons in another Los Alamos Van de Graaff generator. The same detector, in approximately the same geometry as before, was used for these measurements (curves *B* on Figs. 1 and 2). It is seen (a) that the 1.06-Mev peak does not occur in the F^{20} spectrum, and (b) that the decay of the 1.63-Mev γ ray from the pure F^{20} is slightly steeper than that from the O^{20}-F^{20} mixture. [$\tau_{1/2}(F^{20}) = 11.2 \pm 0.1$ sec.] This confirms our tentative assumption stated above.

A computer analysis of the decay curves obtained from the O^{20}-F^{20} mixture, analyzed on the basis of a single activity plus a background, yielded apparent half-lives of 12.4 ± 0.1 sec for the 1.06-Mev peak and 12.1 ± 0.1 sec for the 1.63-Mev peak. As is evident from Fig. 2, the decay curve of the 1.63-Mev peak from the O^{20}-F^{20} mixture closely approximates a straight line. The data were further analyzed, however, by

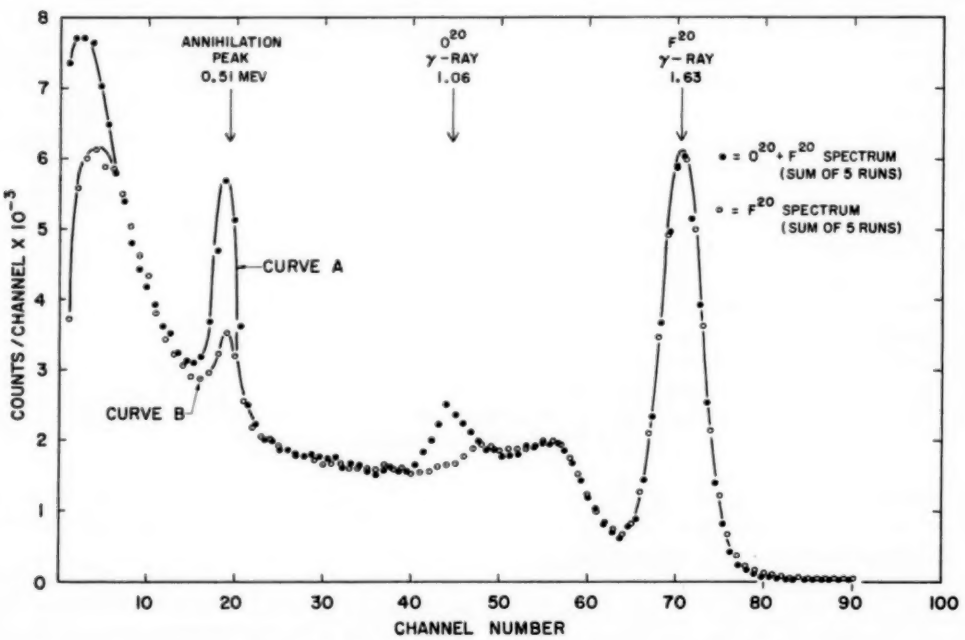

FIG. 1. Scintillation spectra obtained following the bombardment of O^{18} (95% enriched) with tritons (Curve *A*) and F^{19} with deuterons (Curve *B*). The annihilation peak is due to positrons from 1.87-hr F^{18}, formed by the reaction $O^{16}(t,n)$.

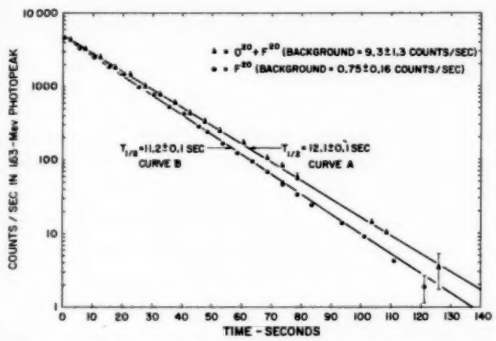
COUNTS / SEC IN 1.63-Mev PHOTOPEAK
TIME - SECONDS
▲ = O20 + F20 (BACKGROUND = 9.3±1.3 COUNTS/SEC)
● = F20 (BACKGROUND = 0.75±0.16 COUNTS/SEC)
T1/2 = 11.2±0.1 SEC
CURVE B
T1/2 = 12.1±0.1 SEC
CURVE A

FIG. 2. Decay of the 1.63-Mev γ ray. The lines are based on an IBM-704 least-squares fit of the data which have been corrected for background.

fitting them to the decay of two—partly genetically related—activities plus a background, using the measured F^{20} half-life of 11.2 sec as one of the activities. This analysis yielded a value for the O^{20} half-life of 13.6 ± 1.0 sec.

The amount of O^{20} relative to F^{20} produced in the target was deduced from this analysis and also calculated independently from the $O^{20} + F^{20}$ spectrum (Fig. 1, Curve *A*). The validity of the analysis using two activities plus a background is substantiated by the good agreement between these two values, $6.2 \pm 3.5\%$ and $5.8 \pm 1.0\%$, respectively.

Figure 3 shows the proposed decay scheme of O^{20}. From the values for $\tau_{1/2}(O^{20})$ and for $E_{\beta max}(O^{20}) = (3.75 - 1.06)$ Mev $= 2.69$ Mev, we compute $\log ft = 3.77$. The analysis of the stripping reaction $F^{19}(d,p)F^{20}$ has shown[5] that the 1.06-Mev state in F^{20} is either 1+ or 0+. The low $\log ft$ value for the beta transition from O^{20} ($I = 0$, even) to the 1.06-Mev state indicates that the transition is of the Gamow-Teller type, as a Fermi transition with $\Delta T = 1$ is forbidden. Hence we conclude that the 1.06-Mev state in F^{20} is 1+.

We wish to thank Dr. A. Schardt for his generous advice and help given during the course of this experiment. One of us (G. S.-G.) should like to thank the staff of Los Alamos Scientific Laboratory for their hospitality.

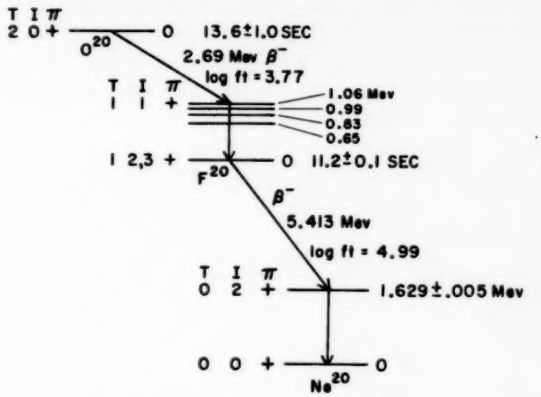

FIG. 3. Proposed decay scheme for O^{20}. The excited states of F^{20} and the decay scheme of F^{20} are taken over from reference 5. The spin and parity assignment of the 1.06-Mev state results from the present work.

---

†Work performed under the auspices of the U. S. Atomic Energy Commission.

[1]N. Jarmie and M. G. Silbert, Phys. Rev. Letters 3, 50 (1959).

[2]Sheline, Campbell, and Peele, Oak Ridge National Laboratory Report ORNL-1798, 1954 (unpublished).

[3]S. Katcoff and J. Hudis, J. Inorg. Nuclear Chem. 3, 253 (1956).

[4]S. Amiel and R. E. Segel, J. Inorg. Nuclear Chem. 10, 4 (1959).

[5]F. Ajzenberg-Selove and T. Lauritsen, Nuclear Phys. 11, 1 (1959).

[6]Amiel and Segel (reference 4) "observed the possible presence of a weak γ ray of 1.1 Mev and a half-life of 13.5 sec for the decay of the 1.63-Mev γ ray, somewhat higher than but consistent with the 11.4-sec half-life" reported for F^{20}. They did not pursue the problem further.

OBSERVATIONS ON THE MÖSSBAUER EFFECT IN Fe^{57}†

S. S. Hanna, J. Heberle, C. Littlejohn, G. J. Perlow, R. S. Preston, and D. H. Vincent
Argonne National Laboratory, Lemont, Illinois
(Received December 2, 1959)

The recent observation[1] of a large resonant absorption of gamma rays by the 14-kev level of Fe^{57} at room temperature has led to a subsequent study of the phenomenon in this laboratory. Because of the various interesting possibilities which this effect provides for further experimentation,[1,2] we present here some preliminary results of our investigation.

We have measured the magnitude of the Mössbauer absorption[3] for sources and absorbers in metallic form or as compounds, at room temperature and also when cooled with liquid nitrogen. These observations are summarized in Table I in which the tabulated entries indicate the observed absorption at resonance. The metal sources were prepared by co-plating iron and radioactive Co^{57} from a weak sulfuric acid solution. The Co^{57} was obtained by deuteron bombardment of iron followed by a separation[4] of inactive iron by ether extraction of $FeCl_3$. To insure the electrodeposition of a good metallic iron film on copper, an appropriate amount of $FeSO_4$ was added to the solution. The metal absorbers were usually rolled metal foils either of natural iron or of iron enriched to 76% in Fe^{57}. The thinnest rolled foil was approximately 60 microinches thick. Thinner absorbers were obtained by electroplating Fe^{57} upon thin copper foils Sources and absorbers in the form of ferrous sulfate were prepared by allowing a solution of the material to evaporate on a suitable backing.

Table 1. Maximum resonant absorption in percent for various combinations of sources and absorbers. The metal absorber is 2.5 mg/cm² of Fe^{57}. The metal source is a Co-Fe plated film. The salt is $FeSO_4 \cdot 7H_2O$. The symbols (RT) and (LT) stand for room temperature and low temperature, respectively. The estimated error in the numbers is about ± 5. The salt absorbers were made with enriched iron.

	Absorber		
Source	Metal (RT)	Metal (LT)	Salt (RT)
Metal (RT)	52		
Metal (LT)		75	
Salt (RT)	~0		4
Salt (LT)	10		8

For a given source and absorber, the resonant absorption was obtained by measuring the transmission with the source and absorber clamped firmly in a rigid container and comparing it with the transmission obtained when the source or the absorber was vibrating at high frequency and small amplitude. Vibration was produced by coupling to the voice coil of a loudspeaker. The absorbing foils were clamped between two disks of beryllium metal in order to obtain the necessary rigidity without undue attenuation of the counting rate. A source or an absorber could be cooled by attaching it in an evacuated space to the bottom of a metal can filled with liquid nitrogen.

It is apparent from Table I that the largest absorption at a given temperature is obtained with a metal source and a metal absorber. A Mössbauer absorption is also observed, however, for nonmetallic samples and this absorption is greatly enhanced at low temperature. Of particular note is the relatively large absorption (~10%) that is observed with the ferrous source and the ferromagnetic absorber. All of these observations suggest that the environment in the source or in the absorber plays a major role through its influence on the Debye temperature of the substance. The effect of environment on the expected hyperfine splitting of the nuclear levels,[1] on the other hand, is not sufficiently large to eliminate the resonant absorption.

In order to obtain a measure of the total strength of the absorption in the case of a metal source and a metal absorber, both at room temperature, the transmission was measured as a function of the relative velocity between source and absorber. In this work the source and the detector were mounted securely on the axis of a Monarch Model *EE* lathe and the absorber was attached to the carriage which provided apparently uniform velocities as small as 10 microns per second. Transmission curves obtained with this arrangement are shown in Fig. 1 for three different thicknesses of absorber. It is seen that the transmission curves are symmetric around zero velocity within the accuracy of the measurements. Furthermore, the fact that the areas in the transmission dips are approximately proportional to the square root of the thickness of absorber indicates that the absorbers are

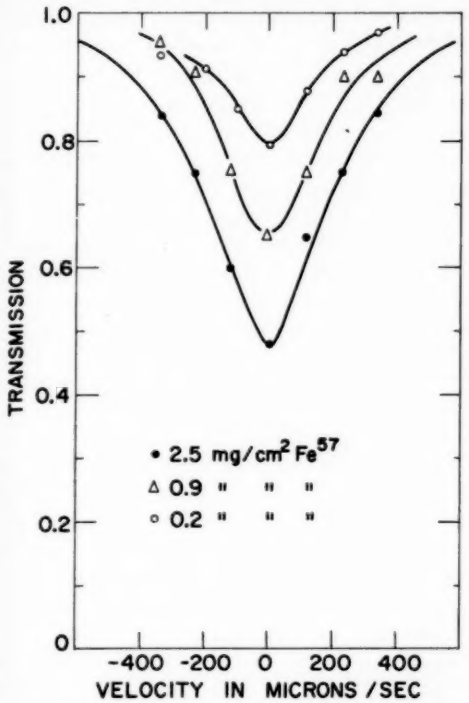

FIG. 1. Transmission curves obtained with a Co^{57} source electroplated in an iron metal environment and iron metal absorbers enriched to 76% in Fe^{57}. The two thicker absorbers were rolled foils; the thinnest sample was a film electroplated on copper. The curves are normalized to the transmission at "infinite" velocity, i.e., the transmission obtained when either the source or the absorber was vibrated at high frequency.

"thick." If one makes the simplifying but rough assumption that the fraction of nuclei in the source which emit without recoil is approximately equal to the fraction in the absorber which absorb without recoil, analysis of these curves by the area method gives a value of 0.6 for this fraction. This number is in good agreement with the theoretical value of 0.7 calculated[2] for room temperature. The measured cross section for absorption of gamma rays at resonance turns out to be approximately 1.4 megabarns, which is roughly 300 times as large as the electronic absorption per atom. An internal conversion coefficient of approximately 10 has been assumed in obtaining the cross section.[5]

The empirical widths of the transmission dips are about twice the width expected from the natural line breadth[5] (4.5×10^{-9} ev) which confirms the thick nature of the absorbers. A detailed analysis of empirical width as a function of absorber thickness with a more refined calculation of the emitting and absorbing fractions is not attempted here because of incomplete knowledge of the instrumental resolution function. There is in fact evidence in our observations that the width of the transmission dip is influenced by the environment of the emitter or the absorber, but clarification of this point must await further experimentation.

Not shown in Fig. 1 is a curve obtained with a 1-mil absorber of natural iron (2.2% Fe^{57}). The ease with which this curve was obtained confirms the qualitative fact that the nuclear cross section is indeed many times the electronic cross section.

We wish to thank M. Hamermesh for constant encouragement and valuable discussion, and Mina Rea Perlow for her expert and generous assistance in all phases of the chemical preparations.

---

†Work performed under the auspices of the U. S. Atomic Energy Commission.

[1]J. Schiffer and W. Marshall, Phys. Rev. Letters 3, 556 (1959).

[2]R. V. Pound and G. A. Rebka, Phys. Rev. Letters 3, 439 (1959).

[3]R. L. Mössbauer, Z. Physik 151, 124 (1958); Naturwissenschaften 45, 538 (1958); Z. Naturforsch. 14a, 211 (1959).

[4]Collected Radiochemical Procedures, Los Alamos Scientific Laboratory Report LA-1556 (unpublished).

[5]Nuclear Levels Schemes, $A=40 \rightarrow A=92$, compiled by Way, King, McGinnis, and Van Lieshout, U. S. Atomic Energy Commission Report TID-5300 (U. S. Government Printing Office, Washington, D. C. 1955).

π^+-p SCATTERING AND PHASE-SHIFT ANALYSIS AT 310 Mev*

James H. Foote, Owen Chamberlain, Ernest H. Rogers, Herbert M. Steiner, Clyde Wiegand, and Tom Ypsilantis

Lawrence Radiation Laboratory, University of California, Berkeley, California
(Received November 30, 1959)

In an experimental program recently completed at the 184-inch synchrocyclotron in Berkeley, data were obtained on elastic π^+-p scattering at a laboratory energy of 310 Mev. Quantities measured were the differential cross section, the total cross section, and the polarization of the recoil protons as a function of center-of-mass angle. We have analyzed the data in terms of S, P, and D waves and have obtained only one acceptable solution. The resultant set of phase shifts is of the Fermi type. The D-wave phase shifts are small but definitely needed to obtain an adequate fit to the data.[1] Owing to the relatively high accuracy of the cross-section data and the inclusion of the results of the polarization experiment, the errors on the small phase shifts have been reduced to less than 1°. The differential-cross-section and polarization data are given in Tables I and II.

Table I. Experimental differential-cross-section measurements. Statistical and independent systematic errors are included. Not shown is an error of +7% and -5% in the absolute differential-cross-section scale.

$\theta_{\text{c.m.}}$ (deg)	$(d\sigma/d\Omega)_{\text{c.m.}}$ (mb)
34.5	12.80 ± 0.35
36.3	12.07 ± 0.45
43.9	10.11 ± 0.25
56.6	7.62 ± 0.25
59.8	6.67 ± 0.20
69.1	4.84 ± 0.14
74.9	3.78 ± 0.12
81.2	2.96 ± 0.13
97.6	1.77 ± 0.10
107.8	1.71 ± 0.07
120.9	2.21 ± 0.09
135.0	3.00 ± 0.19
144.5	3.81 ± 0.16
151.9	4.12 ± 0.33
156.0	4.57 ± 0.18
165.2	4.96 ± 0.20

We performed the phase shift analysis with the aid of an IBM 704 electronic computer, using a search program that obtained a least-squares fit to the data.[2] The computer was able to accept and vary a set of phase shifts until it had located a relative minimum for the quantity M, where

$$M = \sum_i [(X_i^{(c)} - X_i^{(e)})/\sigma_i(e)]^2.$$

Here $X_i^{(e)}$ = the quantity X_i as obtained from experiment, $\sigma_i^{(e)}$ = the experimental error (standard deviation) on $X_i^{(e)}$, and $X_i^{(c)}$ = the quantity X_i as calculated by the computer from a given set of phase shifts. The sum is taken over all the experimental quantities.

Table II. Experimental measurements of the polarization P of the recoil protons. All errors are shown and are assumed independent. The sign of the polarization is said to be positive when a preponderance of the recoil protons have their spins pointing in the direction of $\vec{p}_i \times \vec{p}_f$, where this quantity is the cross product of the initial and final momentum vectors of the π mesons.

$\theta_{\text{c.m.}}$ (deg)	P
113.5	+0.053 ± 0.078
124.0	-0.198 ± 0.075
133.5	-0.189 ± 0.063
145.5	-0.185 ± 0.055

In order to obtain every minimum that might lie in the neighborhood of the true solution, random sets of phase shifts were fed into the computer and the resultant fits examined. From 244 random sets, 27 unique clusters of solutions were found. The solutions in each cluster agreed to within a few tenths of a degree in every phase shift. All the 27 minima were obtained at least five times (except for a few with very large M values). Assuming that the relative minima are randomly spaced and can be entered with

equal ease, the probability of having missed an acceptable set is less than 1%.

Early in the analysis it became evident that a good fit to the data could not be obtained by using S and P waves only. Thus, D waves were also allowed in the random search while the phase shifts relating to higher-order orbital angular-momentum states were assumed negligible. Coulomb scattering was included in the analysis by assuming that the nuclear and Coulomb phase shifts could be added to give a total phase shift.[3]

Of the 27 solutions found in the random search, all but five have negligible probabilities of lying in the vicinity of the true solution. This conclusion assumes that the errors on the experimental points are independent and normally distributed so that the M values of the solutions are statistically significant. The five possible solutions are presented in Table III. The corresponding curves of the differential cross section and polarization are given in Figs. 1 and 2. Also shown is the inadequate fit with only S and P waves.

Of these five solutions, all but solution a can be eliminated. Our recent experimental differential-cross-section data at small angles (not included in the random search or listed in Table I) definitely indicate that the interference between the Coulomb and nuclear scattering is constructive. This rules out solutions b and e. Set c is of the Minami type and is unreasonable because of its large δ_{33}, the low-energy behavior of its phase shifts, and its disagreement with the requirements of the dispersion relations.[4] This leaves only solutions a (Fermi type) and d (Yang type). When tentative values of the recently obtained cross-section data are included in the analysis, the Yang set is found to be approximately 1/10 as probable as the Fermi set. Furthermore, the Yang-type solution does not satisfy the dispersion relations.[5] We therefore conclude that a is the only allowed solution.

The errors (standard deviations) associated with this solution were derived from the error matrix and are presented in Table IV. The lack of knowledge of the total inelastic cross section at this energy results in additional uncertainty in the phase shifts. Using recent theoretical[6] and experimental[7] results concerning pion production by pions, we estimate that the total inelastic cross section at 310 Mev is less than 1 millibarn. Even this small amount of inelastic scattering can cause variations in the phase shifts listed in Table III. However, our calculations indicate that these changes would probably be within the limits set by the errors in Table IV.

We can compare our final set of phase shifts with the results of other experiments and with

Table IV. The errors (standard deviations) in the phase shifts of solution a. The data in Tables I and II were used to obtain these errors.

Phase shift	α_3	α_{31}	α_{33}	δ_{33}	δ_{35}
Error (deg)	1.2	0.8	1.7	0.5	0.6

Table III. The statistically probable solutions found in the random search. They were obtained by using the data in Tables I and II. The orbital and total angular momentum states represented by each shift are also given. The last column refers to the types of solutions that can arise in this kind of analysis.

Solution	Nuclear phase shifts (deg)					M	Type of solution
	α_3	α_{31}	α_{33}	δ_{33}	δ_{35}		
	($L=0$	1	1	2	2)		
	($J=1/2$	1/2	3/2	3/2	5/2)		
a	-17.7	-3.5	133.2	2.4	-5.0	7.1	Fermi
b	23.2	-119.8	-158.2	-2.2	3.0	11.9	Similar to d except all signs reversed.
c	-6.4	-22.6	-2.1	134.1	0.9	20.2	Minami
d	-23.2	121.9	158.3	8.0	-5.0	25.0	Yang
e	24.0	8.0	-134.6	3.1	-0.4	25.2	Similar to a except that signs of S- and P-wave shifts are reversed.

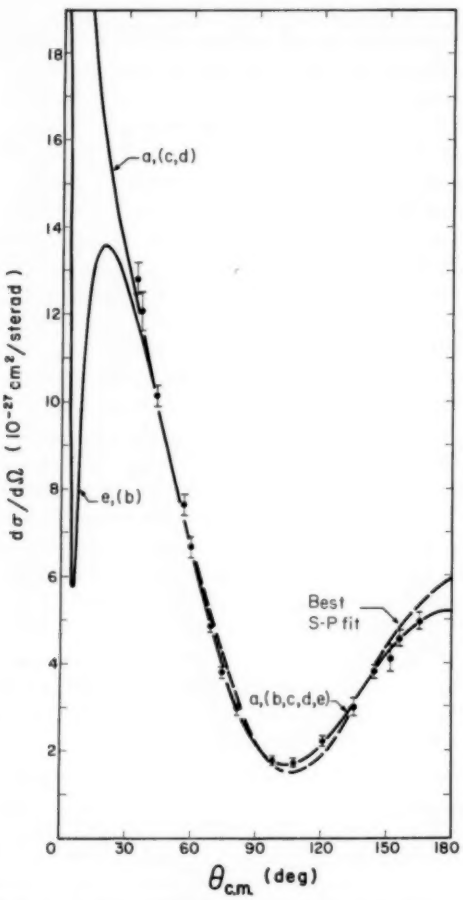

FIG. 1. Experimental differential-cross-section measurements given in Table I. Solid curves represent the S-P-D phase-shift fits to the data as determined by the solutions in Table III. Shown in the figure are the entire curve for solution a and the small-angle behavior of solution e. Letters in parentheses indicate solutions that give curves very similar to the ones plotted. The Minami (c) and Yang (d) solutions are slightly poorer fits to the data than is the Fermi (a). The S-P fit is shown only in the region where it noticeably deviates from the data.

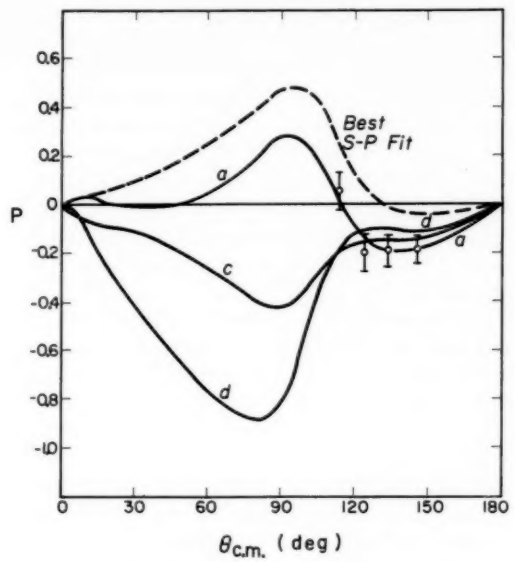

FIG. 2. Experimental recoil-proton polarization measurements given in Table II. Solid curves represent the S-P-D phase-shift fits to the data as determined by the solutions in Table III. To avoid confusion, sets b and e are not shown; they give results similar to curves a and c, respectively. The best S-P fit is indicated by the dashed curve.

theory. The real part of the forward elastic scattering amplitude, calculated by using solution a, agrees with the results of the dispersion relations when the value of 0.08 is used for the renormalized, unrationalized, pion-nucleon coupling constant.[8] Our value of α_{33} is consistent with other experiments at energies above the resonance region in that it also falls below the straight line passing through the low-energy points on a Chew-Low plot.[9] The small P-wave phase shift α_{31} is now known quite accurately at 310 Mev. Its sign is negative, in agreement with the effective-range approach of Chew and Low[9] and with other experimental results.[10] The S-wave phase shift α_3 has a more negative value than is indicated by a linear extrapolation of the low-energy data, but the discrepancy is not so great as that found when only S and P waves are allowed.

Finally, we compare our experimentally determined D-wave phase shifts with the predictions of Chew, Goldberger, Low, and Nambu[11] based on the dispersion relations. They predict $\delta_{33} = 0.3°$ and $\delta_{35} = -2.5°$ at our energy. Chew[12] estimates that the errors introduced in these theoretically calculated phase shifts should be less than 30% if one assumes that the effects of the pion-pion interaction are negligible. Thus the differences between our D-wave phase shifts and those obtained from theory suggest that the pion-pion interaction may be significant in describing pion-nucleon scattering.

We would like to acknowledge the invaluable assistance given us during the experimental work by Mr. James T. Vale and the rest of the 184-inch cyclotron personnel. We greatly appreciate suggestions concerning the phase-shift analysis by Mr. Kent K. Curtis and Mr. Edwin M. Towster of the Mathematical and Computing Section of the Theoretical Group.

*This work was performed under the auspices of the U. S. Atomic Energy Commission.

[1]The D-wave phase shifts agree with those found by E. L. Grigoriev and N. A. Mitin at 307 Mev. See B. Pontecorvo, Proceedings of 1959 International Conference on Physics of High-Energy Particles, Kiev (unpublished), p. 35.

[2]The experimental methods used to obtain the data given here and the details of the analysis will be described fully in the Physical Review at a later date. Data recently obtained on the small-angle differential cross section and the total cross section will also be presented then, along with the completed analysis. When these recently obtained data are included, the errors on all the phase shifts are expected to be less than 1°.

[3]This method of including Coulomb scattering is essentially that used by Stapp, Ypsilantis, and Metropolis, Phys. Rev. 105, 302 (1957). First order relativistic corrections to the Coulomb shifts were obtained using formulas (3) of F. T. Solmitz, Phys. Rev. 94, 1799 (1954). Discussions with Dr. Stapp clarifying the Coulomb scattering problem are gratefully acknowledged.

[4]S. J. Lindenbaum and R. M. Sternheimer, Phys. Rev. 110, 1174 (1958).

[5]W. C. Davidon and M. L. Goldberger, Phys. Rev. 104, 1119 (1956); W. Gilbert and G. R. Screaton, Phys. Rev. 104, 1758 (1956).

[6]L. S. Rodberg, Phys. Rev. Letters 3, 58 (1959).

[7]W. J. Willis, Phys. Rev. 116, 753 (1959).

[8]T. D. Spearman (to be published).

[9]G. F. Chew and F. E. Low, Phys. Rev. 101, 1570 (1956).

[10]For example, Mukhin, Ozerov, Pontecorvo, Grigoriev, and Mitin, Proceedings of the CERN Symposium on High-Energy Accelerators and Pion Physics, Geneva, 1956 (European Organization of Nuclear Research, Geneva, 1956), Vol. II, p. 221.

[11]Chew, Goldberger, Low, and Nambu, Phys. Rev. 106, 1337 (1957).

[12]We wish to thank Professor Chew for several enlightening discussions.

POLARIZATION OF Λ^0 FROM PHOTOPRODUCTION IN HYDROGEN*

B. D. McDaniel,† P. Joos,‡ D. McLeod,‖ S. Richart,‖ and D. Zipoy**
Cornell University, Ithaca, New York
(Received November 30, 1959)

We have studied the reaction $\gamma+p\rightarrow K^+ + \Lambda^0$, searching for a polarization of the Λ^0 with respect to the production plane. The polarization is analyzed by means of the asymmetric decay,[1] $\Lambda^0\rightarrow p+\pi^-$. The K meson and the decay proton are detected in coincidence.

The experimental arrangement is shown in Figs. 1 and 2. The K detection is quite similar to that used earlier in this laboratory.[2] The Cornell synchrotron operating at 1080 Mev produces a bremsstrahlung beam which is collimated to a diameter of one inch as it passes through a cylindrical liquid hydrogen target of 3-inch length. K mesons, which are produced

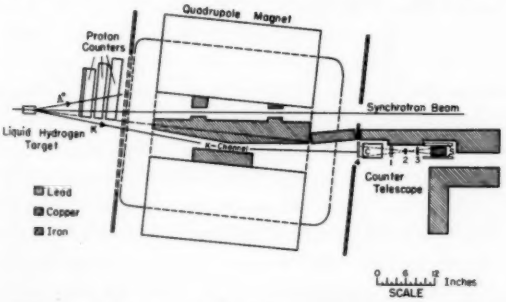

FIG. 1. Top view of target and quadrupole analyzing magnet.

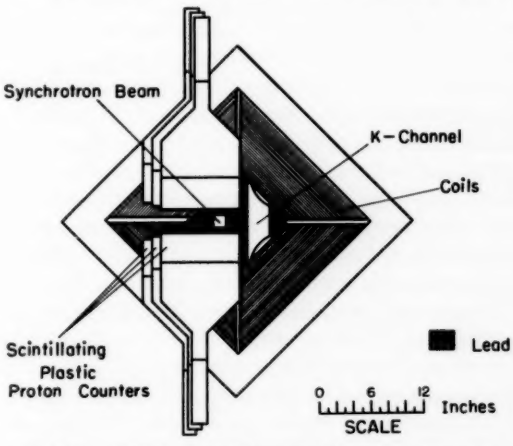

FIG. 2. Front view of magnet showing entrance channel for K particles and the two sets of proton counters, consisting of three counters each.

in the target, are magnetically selected in the momentum interval of 515 ± 60 Mev/c by using one side of a quadrupole magnet and a counter telescope. The magnet accepts K mesons at an angle of $9.8^{+1.8}_{-0.8}$ deg with respect to the beam which corresponds to a center-of-mass angle of 32^{+10}_{-6} deg. These kinematical conditions correspond to production by photons of 1000 ± 30 Mev. The requirement for the selection of a K particle is a coincidence between scintillation counters 1, 2, 3, 4 and the side counters, S, which detect the decay particles, together with the Čerenkov counter, C, in anticoincidence.

Most of the Λ^0 particles, emitted at about 12° from the beam, decay while still in the hydrogen target. The decay protons, of energy between 50 and 150 Mev, are emitted within a forward cone of 26°. About one half of these enter one or the other of the two banks of counters, consisting of three counters each, located symmetrically above and below the median plane. A coincidence, with 8-nanosecond resolving time (1 nanosecond $\equiv 10^{-9}$ sec), is taken between each proton counter and the K telescope counter, 1, and this coincidence together with a "K-meson event" is interpreted as the correlated detection of a K meson and an associated decaying Λ^0 hyperon. To compensate for any asymmetries between the two banks of proton counters, they were reversed top for bottom seven times during the run.

The bremsstrahlung beam passes within $1\frac{1}{2}$ inches of the edge of the proton counters, which are shielded by only $\frac{1}{2}$ inch of Lucite; thus the spray of electrons from the target causes an extremely high counting rate in the proton counters. Any proton of energy between 50 and 150 Mev loses at least 40 Mev in one or more scintillation counter, whose thickness is 2 inches. This is four times the energy loss of a minimum-ionizing particle; thus the pulse-height discrimination, which is performed by a biased diode at the output of the photomultiplier tube, can be made at this level, giving good discrimination against electrons. Biases were determined for the proton counters by placing them individually in front of the aperture of the K channel of the magnet and observing the pulse height produced by protons of suitable energy, which were selected by the magnet and telescope.

The background in the K telescope was measured by operating with the peak beam energy below the K production threshold. Though the background measured this way was found to be rather high (60%), the requirement of a simultaneous count in the proton counter provided another large factor of discrimination in favor of the detection of $K^+ - \Lambda^0$ coincidences. The accidental coincidence rate was measured both directly, by counting delayed coincidences between the K telescope and the proton counters, and also by artificially simulating a high rate of K events, through a reduction of the coincidence requirements for the K channel, to obtain a measure of the effective resolution of the system. The background correction for accidental coincidences was about 14%. Measurements of the background rate of normal coincidences both below threshold and without hydrogen were made to make sure the coincidences were indeed due to $K^+ - \Lambda^0$ production.

If we assume the spin of the Λ^0 to have the value $\frac{1}{2}$, and to have a proton decay distribution of the form $(1+\alpha \cos\theta)$, where θ is the angle of emission of the proton with respect to the spin direction and α is the coefficient of parity nonconservation, and if we assume a component of polarization of the Λ^0 in the direction $\vec{p}_K \times \vec{p}_\Lambda$, where $\vec{p}_K$ and $\vec{p}_\Lambda$ are the momentum of the K and Λ particles, then from the geometrical configuration, kinematics, and momentum acceptance of the magnet, we obtain

$$\alpha P_{32^\circ} = 1.41(N_u - N_d)/(N_u + N_d),$$

where P_{32° is the polarization of the Λ° for the center-of-mass production angle of 32°, and N_u and N_d are the number of counts obtained above and below the plane of production. The total number of observed events was 245. After background corrections, one obtains the value $\alpha P_{32^\circ} = 0.04 \pm 0.11$. The error indicated is purely statistical. Any systematic errors due to misalignment of the apparatus are estimated to be much smaller than this.

If one uses the value,[3] $\alpha > 0.73 \pm 0.14$, we would then find $P_{32^\circ} < 0.05 \pm 0.15$. This value may be compared with that obtained assuming only s and p states contribute to the production near threshold, in which case the polarization should be proportional to the sine of the production angle measured in the center-of-mass system, thus giving a maximum polarization equal to 0.53 for the angle of 32°. Our failure to observe an asymmetry, together with the near isotropy of the cross section and its lack of p^3 dependence near threshold,[2] is consistent with the conclusion that

an s state predominates in the production at this energy.

*Supported in part by the joint program of the Office of Naval Research and the Atomic Energy Commission.

†Now on leave at Laboratorio Nazionale di Frascati, Frascati, Italy.

‡Visiting Fellow on leave from Physikalisches Staatsinstitut, Universität Hamburg, Hamburg, Germany.

‖National Science Foundation Predoctoral Fellow.

**Now at the University of Maryland, College Park, Maryland.

[1]Crawford, Cresti, Good, Stevenson, and Ticho, Phys. Rev. Letters, 2, 115 (1959).

[2]McDaniel, Silverman, Wilson, and Cortellessa, Phys. Rev. Letters 1, 109 (1958); also 1, 263(E) (1958). P. L. Donoho and R. L. Walker, Phys. Rev. 112, 981 (1958).

[3]J. Steinberger, 1958 Annual International Conference on High-Energy Physics at CERN, edited by B. Ferretti (CERN Scientific Information Service, Geneva, 1958), p. 150. F. S. Crawford, 1958 Annual International Conference on High-Energy Physics at CERN, edited by B. Ferretti (CERN Scientific Information Service, Geneva, 1958), p. 323.

ELASTIC SCATTERING OF K^- MESONS BY NUCLEI

P. B. Jones
Clarendon Laboratory, Oxford, England
(Received December 10, 1959)

This note describes a measurement of the small-angle elastic scattering of K^- mesons of energy 144-106 Mev by the nuclei in photographic plates. The experimental reaction cross section and elastic differential cross section have been compared with cross sections obtained by exact numerical solution of the Klein-Gordon equation in which the K^--nucleus optical model potential, $V(r)=(U-iW)f(r)$, is taken to be the fourth component of a relativistic 4-vector. This method of measuring U is more direct and precise than the method based on the energy loss in K^--meson inelastic scattering.[1] We find that the most probable value of U is -30 Mev (i.e., attractive). Using the approximation $V(r)=\rho(r)\langle t\rangle$ (based on the impulse approximation), where $\rho(r)$ is the nuclear density and $\langle t\rangle$ is the K^--nucleon transition matrix for forward scattering, the sign of U depends on the sign of the real part of the K^--proton s-state scattering length,[2] which is of importance in the evaluation of the K-nucleon forward scattering dispersion relations.[3-5]

A stack of 240 pellicles of Ilford $K.5$ nuclear photographic emulsion, each 15×22.5 cm^2 and of 600μ thickness, was exposed to the 435-Mev/c electromagnetically separated K^- beam of the Bevatron at Berkeley. K^--meson tracks were followed for approximately 3.7 cm starting from a plane where the average energy was 144 Mev. For 6.97 meters of track the real angle of scattering was calculated for all elastic scattering events with projected angle $\phi\geq1.5°$. The same procedure was adopted for a further 12.06 meters of track for elastic scattering events with $\phi\geq2.0°$. 23.00 meters of track were scanned for decays in flight and all inelastic events. This gave a mean free path in the energy interval 144-106 Mev of $30.7^{+4.0}_{-3.2}$ cm for all inelastic processes. Combination of this result with results for the same energy interval published by other workers[6,7] gives a mean reaction cross section for the nuclei of photographic plates of 710 ± 44 mb.

For each elastic scattering, the momentum transfer was calculated in addition to a correction factor for solid angle and for the finite resolution of the detecting apparatus. The scattering events were divided into intervals of momentum transfer (q) of 20-25, 25-30, 30-40, 40-50, 50-65, and 65-96 Mev/c. For each interval the experimental value of the mean $d\sigma/dq$ (mb per Mev/c) was calculated. Theoretical values of this quantity and of the mean reaction cross section were calculated by exact numerical solution of the Klein-Gordon equation at a K^- energy of 125 Mev, the emulsion nuclei being represented with only a very small error by nuclei of $A=94$, $Z=41$, and $A=14$, $Z=7$ with weights 0.435 and 0.565. For comparison with the experimental $d\sigma/dq$, the theoretical values were integrated over each of the six intervals of momentum transfer. We assume that $V(r)$ is independent of mass number and choose for $f(r)$ the Saxon-Woods form[8] with $r_0=1.07\,A^{1/3}\times10^{-13}$ cm and diffuseness parameter $a=0.57\times10^{-13}$ cm.

We have obtained eleven sets of the two free parameters U and W ($-60\leq U\leq60$ Mev) which

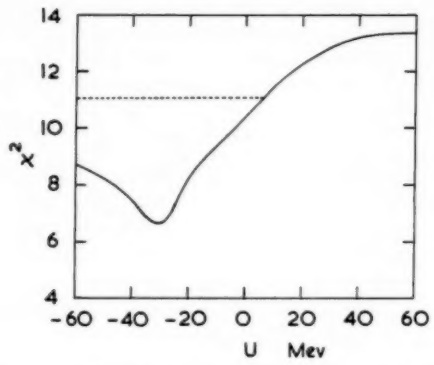

FIG. 1. χ^2 is shown as a function of U. The broken line shows the 5% level of significance.

give a mean reaction cross section of 710 mb. The $d\sigma/dq$ predicted by each set are compared with the experimental values in Fig. 1, which shows the value of the parameter χ^2 as a function of U. The lowest value of χ^2, 6.70 for $U = -30$ Mev, is satisfactory for five degrees of freedom. The 5% level of significance, shown by the horizontal broken line, corresponds to $U = +6$ Mev. In Fig. 2, $Y = (d\sigma/dq)/(d\sigma/dq)_{\text{Rutherford}}$ is shown as a function of q. The experimental points are compared with the values of Y given by the sets (*a*) -30-37*i* Mev, (*b*) +20-52*i* Mev. $d\sigma/dq$ is most sensitive to changes in U for $q \simeq 50$ Mev/c. It is important to note that the experimental correction factor is large (>1.4) only for the points at $q = 22$ and 27 Mev/c. At $q = 50$ Mev/c we may neglect inelastic scattering and Coulomb excitation.

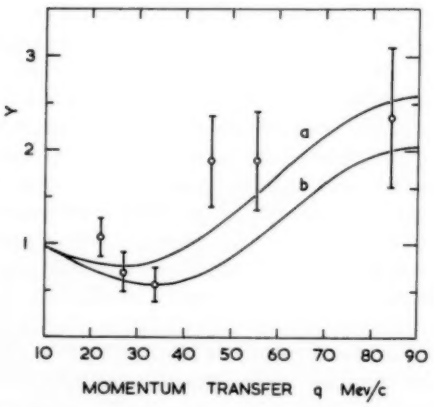

FIG. 2. The experimental values of $(d\sigma/dq)/(d\sigma/dq)_{\text{Rutherford}}$ are compared with those calculated for the potentials (a) -30-37*i* Mev, (b) +20-52*i* Mev.

If the reasonable assumption is made that K^--nucleon p-wave contributions to $\langle t \rangle$ are insufficient to change the sign of U, then the result $U = -30$ Mev agrees with the (a+) and (b+) s-state scattering length solutions of Dalitz and Tuan,[2] but is in poor agreement with the (a-) and (b-) solutions. The value of U at lower K^- energies would be useful, but at 70 Mev, owing[9] to the large value of W, the elastic scattering is almost insensitive to U.

I should like to thank Professor D. H. Wilkinson, F.R.S., for his constant encouragement, Dr. E. J. Lofgren for making the separated K^- beam of the Bevatron available, and Dr. D. J. Prowse for making the irradiation. I should like to thank Miss J. A. Petts for assistance in scanning for the events.

The data analysis and numerical solution of the Klein-Gordon equation were carried out using the Ferranti Mercury digital computer at the University of Oxford Computing Laboratory. The program for the numerical solution of the Klein-Gordon equation was written in collaboration with Dr. P. E. Hodgson.

I should like to thank the Royal Commissioners for the Exhibition of 1851 for a Senior Studentship.

[1]Alles, Biswas, Ceccarelli, and Crussard, Nuovo cimento 6, 517 (1957).

[2]R. H. Dalitz and S. F. Tuan, Ann. Phys. 8, 100 (1959).

[3]P. T. Matthews and A. Salam, Phys. Rev. 110, 565, 569 (1958).

[4]C. Goebel, Phys. Rev. 110, 572 (1958).

[5]K. Igi, Progr. Theoret. Phys. (Kyoto) 19, 238 (1958).

[6]Webb, Iloff, Featherston, Chupp, Goldhaber, and Goldhaber, Nuovo cimento 8, 899 (1958).

[7]Lohrmann, Nikolic, Schneeberger, Waloschek, and Winzeler, Nuovo cimento 7, 163 (1958).

[8]R. D. Woods and D. S. Saxon, Phys. Rev. 95, 577 (1954).

[9]D. H. Stork, Proceedings of the Florida Conference on the Nuclear Optical Model, 1959 (unpublished).

ERRATUM

MAGNETIC DIPOLE RESONANCE OF EXCITED LEVELS IN FREE IONS OF Cd II AND Zn II. Edmond Geneux and Barbara Wanders-Vincenz [Phys. Rev. Letters 3, 422 (1959)].

The authors stated: "We believe that this is the first time that magnetic dipole resonance of free ions has been observed." Professor R. Novick has pointed out to us that one year ago he published an article on an experiment he performed on the He^{3+} ion.[1] It is also well known that Lamb and Skinner have measured the Lamb shift of the He^{4+} ion. Therefore, our sentence was too vague. What we wanted to note is that these resonances seem to be the first ones on ionic levels with allowed transitions to lower energy levels, hence of short lifetime ($\sim 5\times 10^{-7}$ sec).

[1]R. Novick and E. Commins, Phys. Rev. 103, 1897 (1956); 111, 822 (1958).

ABSTRACTS

In this section are printed the abstracts of Articles that have been forwarded to The American Institute of Physics for publication in THE PHYSICAL REVIEW. In quoting information obtained from this section before the appearance of the corresponding Article, reference should be made to "Physical Review (to be published)" rather than to this Journal.

SOME THERMAL PROPERTIES OF LIQUID HELIUM THREE. Louis Goldstein, Los Alamos Scientific Laboratory, University of California, Los Alamos, New Mexico (Received July 6, 1959).

The various anomalies exhibited by the thermal properties of liquid He^3 originate with its nuclear spin system according to the statistical thermodynamic formalism elaborated for the latter. This result of general character is verified directly through a quantitative evaluation of the volume expansion coefficient of the saturated liquid. The theory also yields the explanation of the observed pressure dependence of the temperature locus of its volume anomalies near saturation at moderate pressures. The quantitative extension of the theory into the regions of the compressed liquid and the solid will have to await the forthcoming of precise measurements of several thermal properties in these phases of He^3.

QUANTUM THEORY OF TRANSPORT IN A MAGNETIC FIELD. Petros N. Argyres, Lincoln Laboratory, Massachusetts Institute of Technology, Lexington, Massachusetts (Received June 9, 1959).

A quantum-mechanical theory of transport of charge for an electron gas in a magnetic field is presented that takes account of the quantization of the electron orbits. A transport equation for the necessary elements of the density matrix is developed for arbitrary values of the magnetic field. The scattering is taken to be elastic and is treated only in the Born approximation. The effect of both the magnetic and electric fields on the collisions is taken into account. The influence of the latter has been neglected in previous theories. It is proven, however, to be important in high magnetic fields. It is established that the effect of a transverse electric field on the scattering can be described as the tendency of the electrons to "relax" to a distribution characteristic of thermal equilibrium in the presence of the electric field.

Previous theories of transport for large Hall angles are consistent with this theory. They can be obtained as a special solution, found by iteration, of this transport equation.

The special case of isotropic scattering has been considered in detail.

In this case it is demonstrated that for small enough magnetic fields the usual classical result obtains.

DEVELOPMENT OF SPACE CHARGE AND GROWTH OF IONIZATION IN THE TRANSIENT TOWNSEND DISCHARGE. Yasunori Miyoshi, Nagoya Institute of Technology, Gokiso-Cho, Showa-Ku, Nagoya, Japan (Received November 13, 1958; revised manuscript received September 25, 1959).

By using the general formulas derived from the analysis in a previous paper, calculations are made of the development of electronic and ionic space charges, the growth of space-charge-distorted field, the buildup of current, and the gain in ionization integral due to the field distortion in the transient Townsend discharge. On the basis of these data, two types of Townsend-mechanism spark breakdown are also discussed.

TRANSIENT TEMPERATURE VARIATIONS DURING THE SELF-HEATING OF A PLASMA BY THERMONUCLEAR REACTIONS. Howard D. Greyber,* Radiation Laboratory, University of California, Livermore, California (Received April 3, 1959).

The ion and electron temperature variations in an idealized controlled thermonuclear reactor burning various ratios of deuterium and tritium are calculated. The variation in the fraction of energy deposited to the nuclear and electron gases with temperature is specifically included. One qualitative result is that it would be unsafe to assume nuclear temperature always equal to or greater than electron temperature for a nuclearly reacting plasma with tritium concentration greater than ten percent.

*Now at the General Electric Company, Missile and Space Vehicle Department, Philadelphia, Pennsylvania.

PROPAGATION OF PLASMA WAVES ACROSS A DENSITY DISCONTINUITY. Arnold H. Kritz and David Mintzer, Laboratory of Marine Physics, Yale University, New Haven, Connecticut (Received August 3, 1959).

The linearized plasma equations and the boundary conditions to be satisfied across a surface of density discontinuity are considered. It is shown that an incident longitudinal plasma wave generates reflected and transmitted transverse plasma waves, as well as reflected and transmitted longitudinal waves. The inverse process also occurs. The transverse waves are generated only when the longitudinal wave is almost normally incident; in the inverse process, the generated longitudinal waves are propagated normal to the boundary.

RADIO EMISSION BY PLASMA OSCILLATIONS IN NONUNIFORM PLASMAS. D. A. Tidman, The Enrico Fermi Institute for Nuclear Studies and the Department of Physics, The University of Chicago, Chicago, Illinois (Received January 14, 1959; revised manuscript received October 1, 1959).

Equations of motion for small-amplitude plasma oscillations interacting with the electromagnetic field in slowly varying density or temperature gradients are set up. We then make a calculation of the radio noise excited by a wave packet of plasma oscillations traversing such gradients using the WKB approximation. A similar calculation is also made for a density discontinuity.

EVALUATION OF THERMAL ACTIVATION ENERGIES FROM GLOW CURVES. A. Halperin and A. A. Braner, Department of Physics, The Hebrew University, Jerusalem, Israel (Received August 13, 1959).

A new method for the evaluation of thermal activation energies from glow curves of excited crystals is described. Use is made of the symmetry of the glow peak, from which the activation energy is calculated by a simple formula: $E=(q/\delta)kT_g^2$, where T_g is the peak temperature, k is Boltzmann's constant, δ is the half-width towards the falloff of the glow peak, and q is a factor which can be computed from the shape of the glow peak. Values of $q \leq 1$ were found for monomolecular processes, while $1 \leq q \leq 2$ correspond to bimolecular ones. The method thus enables one to determine the type of kinetics.

THERMAL ACTIVATION ENERGIES IN NaCl AND KCl CRYSTALS. A. Halperin, A. A. Braner, A. Ben-Zvi, and N. Kristianpoller, Department of Physics, The Hebrew University, Jerusalem, Israel (Received August 13, 1959).

Thermal activation energies were computed from various glow peaks of NaCl and KCl single crystals. The method developed in the preceding paper has been used successfully in these calculations. Good agreement was obtained with the results calculated from the initial rise of the glow peaks. Activation energies varied from 0.3 to 1.5 ev for various peaks in the glow curve of NaCl between 150 and 500°K. Similar results were obtained for KCl crystals.

The kinetics of the processes was found to be nearly of first order.

RANGE OF 1-10 kev ELECTRONS IN SOLIDS. Charles Feldman, United States Naval Research Laboratory, Washington, D. C. (Received August 7, 1959).

The range of 1-10 kev electrons in metals and phosphors has been measured by recording the light output as a function of energy from a sample consisting of a metallic layer deposited on a transparent phosphor layer. The measurements lead to the development of the following range-energy expression: $R=250(A/\rho Z^{n/2})E^n$, where $n=1.2/(1-0.29\log_{10}Z)$, E = energy in kev, R = range in angstroms and A, ρ, Z, have their customary meaning. This differs from the usual range expression in the dependence of n on Z. Usually n is assumed to be independent of material. This dependence can be justified on the basis of Bethe's theory of electron stopping power.

MODULATION-EFFECT CORRECTIONS FOR MOMENTS OF MAGNETIC RESONANCE LINE SHAPES. K. Halbach,* Stanford University, Stanford, California (Received August 10, 1959).

Corrections are derived for the calculation of the second and fourth moments of magnetic resonance lines from experimental data, obtained

by using the low-frequency modulation method. The results for 0° phase shift between field modulation and the lock-in reference are

$$\langle \Delta\omega_{\text{exp}}{}^2 \rangle_{\text{Av}} = \langle \Delta\omega^2 \rangle_{\text{Av}} + \tfrac{1}{3}\omega_M{}^2 + \tfrac{1}{4}(\gamma H_M)^2,$$

$$\langle \Delta\omega_{\text{exp}}{}^4 \rangle_{\text{Av}} = \langle \Delta\omega^4 \rangle_{\text{Av}} + \langle \Delta\omega^2 \rangle_{\text{Av}}[2\omega_M{}^2 + \tfrac{3}{2}(\gamma H_M)^2] + \tfrac{1}{5}\omega_M{}^4 + \tfrac{3}{4}\omega_M{}^2(\gamma H_M)^2 + \tfrac{1}{8}(\gamma H_M)^4.$$

Furthermore, it is found that no corrections are necessary for the calculation of intensities despite distortion of the line shape resulting from modulation effects.

The equivalence of field and frequency modulation is proved for signals describable by Bloch's equations and the discussion of the general case strongly supports the general validity of this equivalence.

*This paper was prepared during a leave of absence from the University of Freiburg, Freiburg, Switzerland.

SYMMETRY OF THE LOW-TEMPERATURE PHASE OF BARIUM TITANATE. Etsuro Sawaguchi* and Melvin L. Charters, School of Ceramics, Rutgers, The State University, New Brunswick, New Jersey (Received August 13, 1959).

In order to find the crystal symmetry of $BaTiO_3$ below -80°C, the domain patterns and optical properties were examined using thin (111) plates specially prepared for this purpose. Four kinds of domains have been differentiated; these domains are optically uniaxial. The crystal symmetry proved to be rhombohedral. The effect of a dc field on the domain configuration was studied. Explanations were given for the strange dielectric and optical behavior which had been thought paradoxical.

*On leave of absence from the Electrotechnical Laboratory, Tanashi, Tokyo.

ELASTIC MODULUS OF ISOTOPICALLY-CONCENTRATED LITHIUM. W. M. Robertson* and D. I. Montgomery, Michigan State University, East Lansing, Michigan (Received August 10, 1959; revised manuscript received October 16, 1959).

The effect of isotopic mass on elastic properties of solids was studied by measuring the elastic modulus of isotopically-concentrated polycrystalline specimens of metallic lithium at 25°C. The elastic modulus of lithium-6 (96.1% Li^6, 3.9% Li^7) was found to be $(7.93 \pm 0.21) \times 10^{10}$ dynes/cm², and that of lithium-7 (7.5% Li^6, 92.5% Li^7) $(7.98 \pm 0.33) \times 10^{10}$ dynes/cm². Within the limits of precision of the experiments, the values do not differ. It is concluded that isotopic mass has no effect on static elastic properties other than that arising from the change in lattice constants.

*Present address: Carnegie Institute of Technology, Pittsburgh, Pennsylvania.

ELECTROMAGNETIC PROPERTIES OF INSULATORS. I. Vinay Ambegaokar and Walter Kohn, Department of Physics, Carnegie Institute of Technology, Pittsburgh, Pennsylvania (Received August 3, 1959).

We discuss the response of a perfect insulator to weak external electromagnetic fields of long wavelength from a many-particle point of view. Our method is to treat the Coulomb interaction between all electrons to all orders of perturbation theory and analyze the structure of the corresponding Feynman graphs. As a result of this graphical analysis we are able to show that the response of the many-particle system to long-wavelength external fields of arbitrary polarization is completely described by a single frequency-dependent dielectric constant. In the limit of long wavelengths as well as low frequencies, we also include, in terms of a magnetic permeability, the magnetic effects of an external field on our system.

CALORIMETRIC STUDIES ON ANNEALING QUENCHED-IN DEFECTS IN GOLD. W. DeSorbo, General Electric Research Laboratory, Schenectady, New York (Received August 4, 1959).

Energy evolved on annealing quenched-in defects in gold has been measured with a high-precision, fast-adiabatic, microcalorimeter. The energy can be described by an equation, $\Delta E_T = B\exp(-E_f/kT_Q)$, where ΔE_T is the total energy evolved for a quench from temperature T_Q. B is a constant equal to $(4.5 \pm 1.0) \times 10^4$ cal/g-atom. E_f, the energy of formation of the defect, is equal to 0.97 ± 0.1 ev in good agreement with the value reported by Bauerle and Koehler

from resistometric studies. The activation energy of motion of the defects has a temperature dependence confirming the results obtained resistometrically, i.e., $E_m = 0.73$ and 0.62 ev at $T_Q = 820°C$ and 920°C, respectively. Assuming that the quenched-in defects are single vacancies, the energy measurements can be combined with the resistivity data of Bauerle and Koehler to give the resistivity increase per one atomic percent vacancies, $\Delta\rho_0/(\Delta E_T/E_f)$, using only experimentally derived quantities. This ratio equals $1.8_0 \pm 0.6$ μohm cm/atomic percent. The volume increase of the gold lattice per vacancy determined from the ratio $\Delta\rho_0/(\Delta E_T/E_f)$, and Bauerle and Koehler's relationship between resistivity and fractional volume change during recovery, is $0.5_7 \pm 0.05$ in good agreement with recent theoretical work of Tewordt.

WAVE FUNCTIONS AND EFFECTIVE HAMILTONIAN FOR BLOCH ELECTRONS IN AN ELECTRIC FIELD. Gregory H. Wannier, Bell Telephone Laboratories, Murray Hill, New Jersey (Received August 3, 1959).

Following up an earlier communication, wave functions are constructed which satisfy the Schrödinger equation for a potential which is a sum of a periodic and a uniform field term. The wave functions are Houston modifications of Bloch-type functions; the Bloch functions form an orthogonal set whose members are fully determined except for phase. The theory exhibits them in the form of power series in the field strength; the unmodified Bloch band functions form the zero-order term of that series. The solutions themselves do not allow for a Zener effect, but the fact that they are only given as power series in E may imply that there is a remainder term causing interband transitions; it would have to be asymptotically smaller than any power of E. Instead of constructing time-dependent solutions of the Schrödinger equation, one can take the time-independent functions to construct an effective Hamiltonian for electrons in one band. Certain indeterminacies are attached to this form of representation; it is shown, however, that final physical answers are unique. The study furnishes an incidental proof that $\vec{k}$ space is a finite space consisting in its entirety of what is customarily called the first Brillouin zone. An appendix treats the case of degenerate bands; such bands have singularities in $\vec{k}$ space even in the absence of a field. The difficulty is circumvented by working with a set which is not yet diagonalized but free of singularities; these intermediate functions can be continued as power series in E in the same way as nondegenerate band functions.

CRYSTAL POTENTIAL AND ENERGY BANDS OF SEMICONDUCTORS. II. SELF-CONSISTENT CALCULATIONS FOR CUBIC BORON NITRIDE. Leonard Kleinman and James C. Phillips, Department of Physics, University of California, Berkeley, California (Received August 5, 1959).

A self-consistent crystal potential is constructed for cubic BN. Exchange is included according to the Slater free-electron approximation. The effect of the heteropolar character of the potential is included explicitly in an approximately self-consistent treatment of the valence-electron charge density. The energy gap is found to be about twice that of diamond, consistent with the results of other zinc-blende crystals and their diamond-type analogs. The maximum of valence band and the minimum in the conduction band are at the center and (100) face of the Brillouin zone, respectively. It is suggested that the heteropolar potential splits the valence band into two sub-bands. The lower sub-band width is about 5 ev, while the higher (which contains three times as many states) has a band width of about 4 ev. The energy gap between the sub-bands is about 10 ev. The effect should be common to all zinc-blende crystals and may be observable by soft x-ray emission.

SPECIFIC HEATS OF $NiCl_2 \cdot 6H_2O$ AND $CoCl_2 \cdot 6H_2O$ BETWEEN 1.4° AND 20°K. W. K. Robinson* and S. A. Friedberg, Carnegie Institute of Technology, Pittsburgh, Pennsylvania (Received August 3, 1959).

The specific heats of $NiCl_2 \cdot 6H_2O$ and $CoCl_2 \cdot 6H_2O$ have been measured from 1.4° to 20°K. Lambda-type anomalies were observed at 5.34°K and 2.29°K for $NiCl_2 \cdot 6H_2O$ and $CoCl_2 \cdot 6H_2O$, respectively, associated presumably with antiferromagnetic-paramagnetic transitions. It has been possible in each case to separate out the magnetic contribution to the specific heat and thus to compute the total magnetic entropy gained in the transition from the fully ordered to com-

pletely disordered condition. This quantity was found to be given accurately by $R\ln(2S+1)$ with $S=\frac{1}{2}$ for Co^{++} and $S=1$ for Ni^{++}. Short-range order is particularly pronounced in these substances, the fraction of the total magnetic entropy gained above the Néel point being 0.52 for $CoCl_2\cdot 6H_2O$ and for 0.40 for $NiCl_2\cdot 6H_2O$. Other features of the anomalies are discussed.

*Now at St. Lawrence University, Canton, New York.

TIME-DEPENDENT INTERNAL FRICTION IN ALUMINUM AND MAGNESIUM SINGLE CRYSTALS. R. H. Chambers* and R. Smoluchowski, Carnegie Institute of Technology, Pittsburgh, Pennsylvania (Received August 3, 1959).

Magnesium and aluminum single crystals subjected to varying amounts of oscillatory strain of audio frequency have been investigated by measuring the strain amplitude-dependent complex dynamical-mechanical modulus at audio frequencies as a function of temperature and time. If the amplitude of the applied excitation exceeds a critical breakaway strain, an excited mechanical state is manifested in a modification of the amplitude dependence of the complex modulus. Upon cessation of the excitation, the excited state decays. The decay following short excitation times obeys a $t^{1/3}$ law, becoming a $t^{2/3}$ law as excitation approaches saturation. The short excitation decay rate is found to be governed by an activation energy in the range of 7 - 10 kcal per mole.

The time dependence is considered to be caused by the dispersal and condensation of a pinning atmosphere which has high diffusivity and is easily dispersed by a dislocation segment undergoing pinning interactions with the atmosphere.

*Now at the John Jay Hopkins Laboratory for Pure and Applied Science, General Atomic Division of General Dynamics Corporation, San Diego, California.

ANTIFERROMAGNETIC STRUCTURE OF CrN. L. M. Corliss, N. Elliott, and J. M. Hastings, Chemistry Department, Brookhaven National Laboratory, Upton, New York (Received August 3, 1959).

Chromium nitride, crystallizing with the rock salt structure, has been found to be antiferromagnetic with a Néel point of 0°C. The magnetic ordering scheme, as determined by neutron diffraction, is that of the fourth kind, with moments arranged in double ferromagnetic sheets which alternate along a line parallel to a face diagonal. The structure is orthorhombic below the transition and the space group *Pnma* has been tentatively assigned. The atomic displacements accompanying the distortion have been partially determined from the diffraction data and are discussed in relation to the magnetic structure. A value of $2.4\mu_B$ has been assigned to the Cr moment; the moment direction is parallel to the b axis of the orthorhombic cell (face diagonal of the cube).

PSEUDODIPOLAR ANISOTROPY IN CUBIC FERROMAGNETS AT LOW TEMPERATURES. S. H. Charap and P. R. Weiss,* Physics Department, Rutgers University, New Brunswick, New Jersey (Received November 6, 1958; revised manuscript received August 18, 1959).

The first order anisotropy constant, K_1, of a cubic ferromagnet with spin 1/2 per atom is calculated as a function of temperature at low temperatures. The source of this anisotropy is taken to be the nearest neighbor pseudodipolar spin-spin interaction and the spin wave approach of Dyson is used. It is shown that K_1 varies as the tenth power of the magnetization, itself a function of the temperature. In order to explain the experimental value of K_1 for nickel at $T=0$ the strength of the dipolar interaction must be ~300 times the classical value. Previous calculations by Van Vleck, Van Peipe, and Tessman are compared with the present work on the ground state. Only the work of Van Peipe accounts properly for the exchange and is in complete agreement with the present investigation. The perturbation scheme of Van Peipe is shown to be rigorously correct, the wave function converging to an exponential form.

*Present address: International Business Machines Research Laboratory, Poughkeepsie, New York.

DRIFT VELOCITY OF ELECTRONS IN HELIUM. A. V. Phelps, J. L. Pack, and L. S. Frost, Westinghouse Research Laboratories, Pittsburgh, Pennsylvania (Received August 10, 1959).

The drift velocity of electrons in helium at 300°K has been measured for E/p values between

4×10^{-4} and 40 volt/cm-mm Hg. The data for $E/p<1$ volt/cm-mm Hg were obtained from measurements of electron transit time in a modernized version of the double-shutter tube developed by Bradbury and Nielsen. The data at high E/p were obtained from microwave measurements of the electron density in a positive column of a low-pressure discharge. The measured drift velocities are in good agreement with previous results in the E/p range from 10^{-1} to 3 volt/cm-mm Hg. At E/p less than 3×10^{-3} volt/cm-mm Hg the electrons are essentially in thermal equilibrium with the gas. Margenau's theoretical expression for the drift velocity of electrons in a gas for which the cross section for momentum transfer is independent of electron energy is found to fit the data for $E/p<1$ volt/cm-mm Hg to the accuracy of measurements. The cross section which gives the best fit of the theory to the data is 6×10^{-16} cm^2.

PRESSURE EFFECTS OF HELIUM AND ARGON ON THE FIRST SHARP SERIES DOUBLET OF INDIUM. Shang-Yi Ch'en, Allen Smith, and Makoto Takeo, University of Oregon, Eugene, Oregon (Received February 19, 1959; revised manuscript received August 3, 1959).

The shift, half-width, and asymmetry of the In λ4101 and λ4511 lines produced by various pressures of helium and argon up to 120 atmospheres and the appearance of satellite bands near these lines are described. The entire absorption line contours and the wings of the pressure-broadened lines were studied. The experimental observations were compared with the Anderson-Talman theory at general pressures.

PRODUCTION OF H^- ($1s^2$) BY HYDROGEN ATOM COLLISIONS. Robert A. Mapleton, Geophysics Research Directorate, Air Force Cambridge Research Center, Air Research and Development Command, L. G. Hanscom Field, Bedford, Massachusetts (Received February 2, 1959; revised manuscript received September 22, 1959).

The post matrix element form of Born's approximation is used to calculate the cross section for H^- ($1s^2$) production in hydrogen atom collisions. The Coulomb wave function is approximated by a plane wave and two different wave functions derived by Chandrasekhar, one of which contains the interelectron distance, are used for the H^- state. The value of the cross section obtained with the wave function containing the interelectron distance term is roughly 25% larger than the other cross section. Since the direct and exchange charge transfer amplitudes, $f_S(\theta)$ and $f_S(\pi-\theta)$, are sharply peaked about $\theta=0$ and $\theta=\pi$, respectively, the interference terms are negligible. Thus, only $f_S(\theta)$ has to be calculated to obtain the cross section.

PHOTOELECTRIC EFFECT IN Pb AT HIGH ENERGIES. R. H. Boyer,* The Clarendon Laboratory, Oxford, England (Received March 11, 1958; revised manuscript received June 12, 1959).

A formula for the photoelectric absorption cross section for the K shell is derived using the Furry or Sommerfeld-Maue approximate wave function. The surviving terms at the high-energy limit are given explicitly and the value for the cross section is found for Pb by numerical integration. The exact wave function is rewritten so as to simplify the derivation of the Furry approximation.

*Present address: Westinghouse Research Laboratories, Pittsburgh, Pennsylvania.

MEASUREMENT OF THE TOTAL, DIFFERENTIAL, AND EXCHANGE CROSS SECTIONS FOR THE SCATTERING OF LOW-ENERGY ELECTRONS BY POTASSIUM. Kenneth Rubin, Julius Perel, and Benjamin Bederson, Department of Physics, New York University, University Heights, New York (Received July 9, 1959).

An atomic beam recoil technique has been used to determine the total, Q, differential, $\sigma(\theta)$, and differential exchange, $\sigma_e(\theta)$, cross sections for the scattering of low-energy electrons by potassium. The method consists of observing the angular distribution of atoms scattered from a potassium atomic beam which has been cross fired by an electron beam. Relative values of $\sigma(\theta)$ are then obtained by transforming to electron scattering angles. An inhomogeneous magnet and collimating channel are used as a velocity filter for the atomic beam. Curves representing the variation of $\sigma(\theta)$ with θ between approximately 15° and 60° are presented for various electron

energies between 0.6 and 9.0 ev.

The magnet also serves to polarize the beam. Relative values of $\sigma_e(\theta)$ were determined by observing the amount of depolarization of the beam in the scattering region, using a second inhomogeneous magnet as an analyzer. Over the observed range of angles, exchange accounts for approximately one third of the scattering. Bounds on the total exchange cross section, Q_e, are also tabulated for energies between 0.5 and 4.0 ev. The bounds on Q_e at 0.5 ev are 0.8×10^{-14} cm^2 $<Q_e<1.6\times10^{-14}$ cm^2.

LOW-ENERGY SCATTERING BY A COMPOUND SYSTEM: POSITRONS ON ATOMIC HYDROGEN. Larry Spruch and Leonard Rosenberg, Physics Department, Washington Square College, New York University, New York, New York (Received May 12, 1959).

The formalism, developed by Kato, which gives upper and lower bounds on the phase shift for the scattering of a particle by a center of force has been generalized to apply to scattering by a compound system. Particularly simple and useful results are obtained for the case of zero-energy scattering where no composite bound state exists. As a first example, because of its relative simplicity, the problem of low-energy positron scattering from atomic hydrogen, with zero total orbital angular momentum, is studied. It is shown that at zero energy the ordinary Kohn variational calculation, which ignores second order contributions, provides an upper bound on the scattering length, from which a bound on the cross section is deduced. For nonzero energies a bound on the phase shift may similarly be obtained, but for a fictitious problem with cut-off potentials. If the energy is sufficiently small (less than 3 ev, say) the error thus incurred is expected to be negligibly small. Numerical calculations performed at $k=0$ and $ka_0=0.2$ lead to the result that at these energies the effects of polarization are large enough to cause the positron to be on the whole attracted to the hydrogen atom.

EXCITED LEVELS OF Mn^{56}. N. D'Angelo, Argonne National Laboratory, Lemont, Illinois (Received August 14, 1959).

The half-lives of the first three excited levels of Mn^{56} have been measured by looking at the cascade gamma rays from neutron capture in Mn^{55}. They are found to be 10.7^{+2}_{-3} mμsec, 4.9 $\pm$0.6 mμsec, and $\leq$0.5 mμsec. A fairly plausible assignment of spins and parities to the first, second, and third excited levels of Mn^{56} would seem to be 2^+, 1^+, and 2^+, respectively. The technique described in the paper should be useful in those cases in which excited levels of unstable nuclei cannot be reached through beta decay.

EXCITATION STUDY OF $F^{19}(n,\alpha)N^{16}$ WITH A BaF_2 CRYSTAL. Daniel M. Smith,* Norman A. Bostrom,† and Emmett L. Hudspeth, The University of Texas, Austin, Texas (Received August 10, 1959).

The scintillation properties of crystalline BaF_2 have been investigated. It was found that this substance yields a reasonably well-defined photopeak when exposed to gamma rays from Na^{22}. With DuMont $K1306$ and 6292 photomultipliers, the signals from BaF_2 are about 1/5 to 1/10 as strong as those from NaI(Tl). With a BaF_2 crystal as a target, the excitation function for the $F^{19}(n,\alpha)N^{16}$ reaction was observed in the region from an apparent threshold near 3.2 Mev up to $E_n=6$ Mev. Several new resonances were found in this region. The cross section generally increases with increasing neutron energy, rising from 85 mb at 4.48 Mev to 200 mb near 6 Mev. Absolute accuracy of cross-section measurements was ±15%.

*Now at Oak Ridge National Laboratory, Oak Ridge, Tennessee.

†Now at Texas Nuclear Corporation, Austin, Texas.

ALPHA-ALPHA SCATTERING IN THE ENERGY RANGE 5 TO 9 Mev. C. M. Jones, G. C. Phillips, and Philip D. Miller,* The Rice Institute, Houston, Texas (Received August 13, 1959).

The scattering of alpha particles from helium has been experimentally studied in the energy range 5 to 9 Mev by the measurement of three excitation functions at the center-of-mass angles 30°33′, 54°44′, and 70°7′. A phase-shift analysis has been performed which indicates that only the S- and D-wave phase shifts are necessary to fit the data in this energy region. Only the well-known D state at approximately 2.9 Mev in Be^8 was observed. The D state has been compared to the single-level dispersion theory and level

parameters have been extracted which are compatible with the alpha-particle model of Be^8.

*Now at Oak Ridge National Laboratory, Oak Ridge, Tennessee.

ALPHA-ALPHA SCATTERING AT 7.56 Mev. N. Berk, F. E. Steigert, and G. L. Salinger, Yale University, New Haven, Connecticut (Received August 5, 1959).

Alpha particles scattered from a helium gas target at an incident energy of 7.56 Mev have been observed in nuclear emulsions. The differential cross sections measured can be fitted with phase shifts of $\delta_0 = 70°$ and $\delta_2 = 100°$.

DOUBLE BETA DECAY. Lothar Meichsner, Max-Planck-Institut für Chemie, Mainz, Germany (Received August 11, 1959).

Formulas are given for the probability of double β decay including energy distributions and angular correlations of the emitted electrons according to the theory of Feynman and Gell-Mann. A strong dependence on the change of angular momentum exists. The formulas also exhibit interference between different intermediate states. The half-life of $_{20}Ca_{28}$ is calculated using matrix elements of j-j shell-model configurations. It is found to be $t \sim 10^{17} \ldots 10^{20}$ years. Actually, t will be much greater, since the matrix elements used are those of favored transitions.

RANGE STRAGGLING OF CHARGED PARTICLES IN Be, C, Al, Cu, Pb, AND AIR. R. M. Sternheimer, Brookhaven National Laboratory, Upton, New York (Received August 5, 1959).

The straggling of the range of charged particles due to fluctuations of the ionization loss has been evaluated for six substances (Be, C, Al, Cu, Pb, and air). The calculations extend up to $T/\mu c^2 \sim 100$, where T is the kinetic energy and μ is the mass of the incident particle. At high energies ($T/\mu c^2 \gtrsim 5$), the integral giving the range straggling becomes somewhat dependent on the ratio μ/m, where m is the electron mass. Two separate calculations have therefore been carried out, which apply to protons and μ mesons, respectively. The results for protons can also be used for π and K mesons in the energy range of interest ($T/\mu c^2 \lesssim 5$).

LOW-LYING LEVELS IN P^{30}. S. S. Yamamoto and F. E. Steigert, Yale University, New Haven, Connecticut (Received August 13, 1959).

The reaction $Al^{27}(\alpha, n)P^{30}$ has been studied at 8.15-Mev bombarding energy using nuclear emulsions as detectors. Neutron groups corresponding to Q values of -2.70, -2.96, -3.59, -4.43, and -4.96 Mev were observed. Comparison of the resulting energy level structure in P^{30} with that obtained by other reactions suggests the possible inversion of the two isobaric-spin ground states.

NUCLEAR ORIENTATION OF Mn^{56}. Rudolf W. Bauer and Martin Deutsch, Department of Physics and Laboratory for Nuclear Science, Massachusetts Institute of Technology, Cambridge, Massachusetts (Received August 14, 1959).

The angular distribution and circular polarization of the gamma rays emitted from 2.6-hr Mn^{56}, polarized at low temperatures in cerium magnesium nitrate, have been measured. Comparing the angular distribution results with angular correlation data, it is possible to establish the spins of the 2.65- and 2.98-Mev excited states of Fe^{56} as 2 uniquely. The amplitude mixing ratios $\delta(E2/M1)$ for the 1.81- and 2.13-Mev γ rays are shown to be $+0.11 \pm 0.06$ and -0.27 ± 0.03, respectively. Gamma-ray anisotropies from aligned Mn^{56} in the same cooling salt have been studied; the results are compared with other Mn alignment experiments. From a simultaneous measurement of the angular distribution of the γ rays from polarized Mn^{52} and Mn^{56}, the ratio of the nuclear g values $(g_{52}/g_{56}) = 0.47 \pm 0.05$ has been determined, giving $\mu_{56} = 3.35 \pm 0.35$ nm. The results of the circular polarization experiment determine μ_{56} to be positive.

DIFFERENTIAL AND TOTAL CROSS SECTIONS OF THE $B^{10}(d,p)B^{11}$ REACTION AT LOW DEUTERON ENERGIES. Gordon R. Harrison,* Gail D. Schmidt,† and Cyril D. Curtis,‡ Department of Physics and Astronomy, Vanderbilt University, Nashville, Tennessee (Received June 30, 1959; revised manuscript received September 30, 1959).

Differential cross sections have been obtained for production of the four highest energy proton groups in the $B^{10}(d,p)B^{11}$ reaction at $E_d = 170$ to 250 kev and for the highest energy group at 140 kev. A laboratory angular range from 0° to 140°

was covered by the scintillation spectrometer technique using a thin CsI(Tl) crystal. Gamow plots of the total cross sections yield slopes approximately equal to the value anticipated from the Coulomb barrier penetration factor.

*Now at Sperry Microwave Electronics Company, Clearwater, Florida.

†Now at U. S. Public Health Service, Washington, D.C.

‡Now at Midwestern Universities Research Association, Madison, Wisconsin.

NEW NEUTRON-DEFICIENT ISOTOPE OF CERIUM. William R. Ware* and Edwin O. Wiig, Department of Chemistry, University of Rochester, Rochester, New York (Received April 1, 1959).

Cerium-132, a positron emitter with a half-life of 4.2 ± 0.2 hours, has been identified through its generic relationship to the known daughter nuclide, La^{132}. An activity of 30 minutes half-life and 4.2 Mev maximum positron energy, which may be due to Ce^{131}, was also observed.

*Present address: National Carbon Co., Palma, Ohio.

SEARCH FOR PSEUDOSCALAR INTERACTION IN $\frac{1}{2}+-\frac{1}{2}-$ β-DECAY TRANSITION. S. Cuperman, Department of Nuclear Physics, The Weizmann Institute of Science, Rehovoth, Israel (Received July 27, 1959).

The longitudinal polarization of the electrons emitted by ${}_{81}Tl^{207}(\frac{1}{2}+-\frac{1}{2}-)$ was measured by double Coulomb scattering. Within the experimental error, a $-v/c$ polarization was obtained. In order to deduce the amount of pseudoscalar contributions, one must know the other nuclear matrix elements. They were taken from a theoretical shell-model calculation and a j-j coupling single-particle model. Assuming $C_S = C_T = 0$, two-component neutrino theory [which predicts opposite polarization in the case of (V,A) and P interactions], left-handed neutrino, and time-reversal invariance, as well as a surface distribution of the nuclear charge, one finds that $|x|^2 \lesssim 4.4 \times 10^{-2}$ (if $C_P/C_A > 0$), with $x = -i(C_P/C_A) \times [\int \beta\gamma_5 / \int \vec{\sigma}\cdot\vec{r}]\rho$ (ρ being the nuclear radius).

CROSS SECTIONS FOR THE PRODUCTION OF Cl, K, Ca, AND Sc ISOTOPES IN THE BOMBARDMENT OF Pb AND U WITH 3.0-Bev PROTONS. G. Friedlander and L. Yaffe,* Chemistry Department, Brookhaven National Laboratory, Upton, New York (Received August 5, 1959).

Cross sections for the formation of some nuclides in the mass number range 38-48 in the bombardment of Pb and U with 3.0-Bev protons have been measured. The maximum of the isobaric yield distributions for the nuclides from the Pb bombardment occurs at the stability line, while that from U is somewhat on the neutron-excess side. Total cross sections of 4-5 mb per mass number are deduced from the Pb data leading to a revision of the mass-yield curve in this region as proposed by Wolfgang et al. The cross sections from uranium are approximately twice as large as those from Pb. The data are shown to be consistent with a cascade-fission-evaporation mechanism.

*Permanent address: Department of Chemistry, McGill University, Montreal, Quebec, Canada.

RANGES AND ENERGY-LOSS PROCESSES OF HEAVY IONS IN EMULSION. Harry H. Heckman, Betty L. Perkins, William G. Simon, Frances M. Smith, and Walter H. Barkas, Lawrence Radiation Laboratory, University of California, Berkeley, California (Received August 12, 1959).

The range-energy relation for C, N, O, Ne, and A ions in nuclear-track emulsion has been measured for energies up to 10 Mev/nucleon. The ions, accelerated by the Hilac, were suitably degraded and subsequently analyzed by a 180° double-focusing magnetic spectrometer. The heavy-ion ranges were measured relative to those of alpha particles which were employed to calibrate the instrument. Within the energy interval studied, it has been found that a general expression for the range of a heavy ion is

$$R = (M/z^2)\lambda(\beta) + Mz^{2/3}C_z(\beta/z),$$

where $\lambda(\beta)$ is the range of a particle of proton mass and charge at velocity βc, $C_z(\beta/z)$ is an empirical function that corrects for the extension in range caused by neutralization of the ionic charge as electrons are captured at low velocities, and M and z are the ionic mass and charge in units of the proton. The range data are sufficiently complete and accurate to allow detailed analyses of the rates of energy loss and effective charge of the heavy ions as they come to rest. The relative importance of primary and secondary ionization processes in producing

the taper in the track of a multicharged ion has been studied by examining the ions in emulsions of various sensitivities. Buckling-type distortions of heavily ionizing tracks in strongly developed emulsion are also discussed. The range-energy relation for low-velocity protons is re-examined and an improved range point at 0.585 Mev is reported.

PHOTOPRODUCTION OF NEUTRAL PIONS AT ENERGIES 600 TO 800 Mev. R. M. Worlock,* California Institute of Technology, Pasadena, California (Received August 11, 1959).

The photoproduction of neutral π mesons from hydrogen has been studied at the California Institute of Technology Synchrotron Laboratory by detecting recoil protons from a liquid hydrogen target irradiated by the synchrotron bremsstrahlung beam. The recoil protons were detected by a five-counter telescope. Data were taken at proton laboratory angles of 19°, 30°, 40°, 50°, and 60° at proton energies corresponding to photon energies of 600, 700, and 800 Mev. Angular distribution data are produced at these three energies and fitted with functions of the form $A+B\cos\theta_\pi'+C\cos^2\theta_\pi'$. These functions are qualitatively like those at lower energies; B is small and $-A/C$ is roughly 1.25. The total cross section is found to have a minimum at about 600 Mev, being slightly larger at 700 and 800 Mev.

*Now at Electro-Optical Systems, Inc., Pasadena, California.

CHANGES IN THE DIFFERENTIAL RIGIDITY SPECTRUM OF PRIMARY COSMIC RAYS ASSOCIATED WITH LONG-TERM AND SHORT-TERM INTENSITY VARIATIONS. J. R. Storey, Physics Department, University of Tasmania, Hobart, Tasmania (Received August 3, 1959).

During June and July, 1958, the cosmic-ray nucleonic component was surveyed along the geographic longitude 147.5°E between geographic latitudes 10°S and 44°S ($\lambda=19°$S and 53°S) at atmospheric depth 475 g cm^{-2} with a neutron monitor mounted in an aircraft. This route is substantially the same as one covered during similar surveys in July and August, 1957. The data have been analyzed to yield long-term and short-term changes in the differential rigidity spectrum $j(N)$, for N in the range 2.0 to 9.0 Bv. A power law, $\Delta j(N)\propto N^{-\beta}j(N)$, with $\beta=1.3$, fits the observations for the long-term change between July, 1957, and July, 1958. For a single short-term variation in 1958 the value $\beta=1.2$ was obtained, with evidence that β decreases at higher rigidities ($N>7.0$ Bv). A 1.5° northward shift of the south latitude knee between the two series of flights is reported. Finally, high-latitude intensity variations of the nucleonic component at 475 g cm^{-2} are compared with variations observed with a neutron monitor at Hobart ($\lambda=52°$, 950 g cm^{-2}). A 1.0% change in intensity at Hobart is equivalent to a 1.8 ± 0.3% change at 475 g cm^{-2}, independently of the time scale of the variations.

POSITIVE-PION SCATTERING FROM HYDROGEN AT 24.8 Mev. Douglas Miller and James Ring, Department of Physics and Astronomy, University of Rochester, Rochester, New York (Received August 10, 1959).

An angular distribution for the process $\pi^++p\rightarrow\pi^++p$ has been measured at 24.8 Mev by counter techniques. At this energy the S-wave interaction is larger than the P-wave. Differential cross sections at the three center-of-mass angles, 66°, 92°, and 163.5°, are 0.286 ± 0.028 mb/sterad, 0.458 ± 0.042 mb/sterad, and 0.993 ± 0.120 mb/sterad, respectively. Over 250 hydrogen interactions were observed at each angle.

SCATTERING OF 200-Mev POSITRONS BY ELECTRONS. J. A. Poirier,* D. M. Bernstein,† and Jerome Pine, High-Energy Physics Laboratory, Stanford University, Stanford, California (Received August 10, 1959).

Scattering of positrons by electrons has been investigated by bombarding a beryllium target with 200-Mev positrons and observing the recoil electrons in a diffusion cloud chamber located behind the target. The cloud chamber was in a magnetic field which permitted the yield of recoil electrons to be measured as a function of their energy W. The experiment covered the range $88\leq W\leq200$ Mev. The positron beam also traversed the cloud chamber and the total number of incident positrons was determined by track-counting.

The total electron yield for $88\leq W\leq200$ Mev

is $(11 \pm 9)\%$ below that predicted by the first-order Bhabha theory. This difference cannot be interpreted until radiative corrections to the theory have been evaluated. A calculation of these corrections which is valid for the conditions of this experiment is not available. The shape of the electron energy spectrum is in good agreement with the Bhabha theory, and inconsistent with the theory if annihilation terms are omitted.

*Now at the University of California Lawrence Radiation Laboratory, Berkeley, California.

†Now at the Stanford Research Institute, Menlo Park, California.

POSITIVE-PION PHOTOPRODUCTION NEAR THRESHOLD. G. Jona-Lasinio and H. Munczek,* Istituto di Fisica dell'Università, Roma, Italia, and Istituto Nazionale di Fisica Nucleare, Sezione di Roma, Italia (Received August 4, 1959).

An investigation is made in order to test the compatibility of photoproduction data on positive pions near threshold, with some predictions of dispersion theory. The result is that no real disagreement necessarily exists between these theoretical predictions and our—still uncertain—experimental knowledge.

*On leave of absence from Facultad de Ciencias Exactas and Comision Nacional de la Energia Atomica, Buenos Aires, Argentina.

ELECTRON SCATTERING BY THE QUADRUPOLE CHARGE DISTRIBUTION OF N^{14}. M. K. Pal,* University of Maryland, College Park, Maryland (Received August 14, 1959).

The recent data of Meyer-Berkhout on the elastic scattering of 420-Mev electrons by N^{14} have been analyzed in the first Born approximation. A detailed treatment is given of the effect of the quadrupole charge distribution of the nucleus in causing a filling-up of the diffraction minimum. The intermediate-coupling ground-state wave function of Visscher and Ferrell with an admixture of the spheroidal type of collective wave function, suggested by Fallieros and Ferrell, has been used in calculating the quadrupole form factor. Instead of using the Born approximation monopole form factor, the exact monopole scattering curve computed by Ravenhall from phase-shift analysis has been used. The spin-flip type magnetic scattering has also been calculated and found to be extremely small. The experimental data show the importance of the quadrupole charge scattering in the neighborhood of the diffraction minimum of the monopole scattering. The quadrupole scattering for the intermediate coupling is, however, completely inadequate to explain the observed data. This gives strong evidence for a collective enhancement of the N^{14} quadrupole moment through core deformation. The model of Fallieros and Ferrell, which predicts a total quadrupole moment of 3.07×10^{-26} cm^2 (collective enhancement $= 2.01\times10^{-26}$ cm^2), is found to give a fairly good fit with the data.

*On leave from the Institute of Nuclear Physics, Calcutta, India.

TWO-NUCLEON POTENTIAL FROM PION FIELD THEORY WITH PSEUDOSCALAR COUPLING. Masao Sugawara,* Brookhaven National Laboratory, Upton, New York, and Susumu Okubo,† University of Rochester, Rochester, New York (Received July 30, 1959).

The two-nucleon potential is derived from ps-ps pion field theory, using the Tamm-Dancoff method with the subsequent appropriate renormalization of the two-nucleon amplitude, up to orders of $g^2(p/\kappa)^2$ and $g^4(p/\kappa)$, g^2 being the equivalent ps-pv coupling constant and p, κ the nucleon (relative) momentum and rest mass, respectively. Neglected are the mass and charge renormalizations and the pion-pion scattering term. It is shown that the only quadratic term is $-V_2(\vec{r})(p^2/2\kappa^2)+\text{H.c.}$, where $V_2(\vec{r})$ is the second-order static potenital. All remaining terms of order $g^2(p/\kappa)^2$ are converted, by a canonical transformation, to terms of order $g^4(p/\kappa)$ or a linear combination of a static and an $\vec{L}\cdot\vec{S}$ potential. In the case of ps-ps coupling, in particular, no velocity-dependent potential besides the quadratic one metioned above follows from diagrams of one- and two-pion exchange without nucleon pairs; thus the nucleon-pair diagrams are the only source of an $\vec{L}\cdot\vec{S}$ potential, if there is any, up to the orders considered. The nucleon-pair diagrams are also estimated assuming the effective pion-pair interaction Hamiltonian, the static limit of which agrees with the S-wave static model of Drell et al. The $\vec{L}\cdot\vec{S}$ potential thus obtained has the right sign in the odd state and changes its sign in the even state, while its magnitude seems in both states somewhat too

small. As for the static part of our potential, the new correction $[g^4(\mu/\kappa)]$ cancels out the conventional fourth-order term $[g^4]$ appreciably; the entire static potential becomes quite close to the second-order static potential down to distances of the order of the pion Compton wavelength, except for the central force in the triplet even state. The details are shown on graphs. The *ps*-*pv* coupling case is treated separately in the following paper.

*On leave during the summer of 1959 from Purdue University, Lafayette, Indiana.

†Now at Department of Physics, University of Naples, Naples, Italy.

TWO-NUCLEON POTENTIAL FROM PION FIELD THEORY WITH PSEUDOVECTOR COUPLING. Masao Sugawara,* Brookhaven National Laboratory, Upton, New York, and Susumu Okubo,† University of Rochester, Rochester, New York (Received July 30, 1959).

The two-nucleon potential is derived from *ps*-*pv* pion field theory up to orders $g^2(p/\kappa)^2$ and $g^4(p/\kappa)$, using the method outlined in the preceding paper, where it was applied to *ps*-*ps* theory. It is shown that the only quadratic term is $-V_2(\vec{r})(p^2/2\kappa^2)+\text{H.c.}$ [$V_2(\vec{r})$ is the second-order static potential], just as in the *ps*-*ps* case. The static part is almost the same as the *ps*-*ps* potential. However, a big difference appears in the $\vec{L}\cdot\vec{S}$ potential; because of the difference in kinematical corrections from *ps*-*ps* and *ps*-*pv* vertices, large $\vec{L}\cdot\vec{S}$ potentials result from both one-pion and two-pion exchange diagrams (with no nucleon pairs), though no $\vec{L}\cdot\vec{S}$ potential follows from such diagrams in the case of *ps*-*ps* theory. The entire $\vec{L}\cdot\vec{S}$ potential has the right sign in the odd state and is of the same sign and of larger magnitude [by a factor of two or three] in the even state. We show that this isospin dependence of the $\vec{L}\cdot\vec{S}$ potential is not appreciably modified even if we add, besides the *ps*-*pv* coupling term, two pion-pair terms which are fitted to low-energy S-wave pion-nucleon scattering. This big difference in the $\vec{L}\cdot\vec{S}$ potential could eventually be used to discriminate between the *ps*-*ps* and *ps*-*pv* theories. Various $\vec{L}\cdot\vec{S}$ potentials, theoretical and phenomenological, are shown on graphs for comparison.

*On leave during the summer of 1959 from Purdue University, Lafayette, Indiana.

†Now at Department of Physics, University of Naples, Naples, Italy.

DEUTERON MAGNETIC MOMENT AND MOMENTUM DEPENDENCE OF TWO-NUCLEON POTENTIAL. Masao Sugawara,* Brookhaven National Laboratory, Upton, New York (Received August 12, 1959).

The correction to the deuteron magnetic moment $[\mu_d]$ is calculated, in the manner pointed out by Feshbach, for the potential derived recently by Sugawara and Okubo from pion field theory. This potential includes, besides an $\vec{L}\cdot\vec{S}$ potential, a quadratic term, $-V_2(\vec{r})(p^2/2\kappa^2)+\text{H.c.}$, [$V_2(\vec{r})$ being the second-order static potential, p and κ the nucleon (relative) momentum and rest mass, respectively]. It is shown in particular that this new term gives a positive correction to μ_d. Numerical magnitudes are estimated using phenomenological deuteron wave functions fitted to all known deuteron data, the hard-core radius $[r_C]$ and the D-state probability $[P_D]$ being adjustable parameters. Results are shown graphically as functions of P_D for two values of r_C. It is seen that the corrections depend sensitively on these two parameters. If there were no other appreciable corrections to μ_d than those discussed here, *ps*-*ps* theory would lead to 6% for P_D while μ_d would not be fitted in the *ps*-*pv* case as well as for the Gammel-Thaler potential, since the correction due to the quadratic term is not large enough to cancel the correction due to the $\vec{L}\cdot\vec{S}$ potential.

*On leave of absence during the summer of 1959 from Purdue University, Lafayette, Indiana.

SCATTERING INVOLVING A BOUND STATE. Smio Tani,* Department of Physics, Case Institute of Technology, Cleveland, Ohio (Received July 27, 1959).

Granting that the formation of a bound state is a "sudden" process as compared to the scattering which may be regarded as a process taking place "adiabatically," a formulation of the scattering involving a bound state is discussed, in which an independent set of creation-annihilation operators is introduced for a particle in the bound state. Here appears a subsidiary condition which prevents the system from having an unduly increased number of degrees of freedom. In the case of potential scattering, which is studied in this paper, this subsidiary condition restricts the intermediate states in a multiple-scattering process to states which are orthogonal to the

bound state. This orthogonality condition gives rise to a simple explanation of the theorem concerning the scattering phase shift at zero energy, in which it is stated that when there is one bound state, the scattering phase shift starts with π at zero energy, if it is to go down to zero at extremely high energy.

*Now at the Department of Physics, Washington University, St. Louis, Missouri.